Bushfire CRC Program D1E

Window and Glazing Exposure to Laboratory-Simulated Bushfires

Report to the Bushfire CRC

P.A. Bowditch, A.J. Sargeant, J.E. Leonard and L. Macindoe

Confidential CMIT Doc. 2006–205

May 2006

A Bushfire CRC initiative

Window and Glazing Exposure to Laboratory-Simulated Bushfires

P.A. Bowditch, A.J. Sargeant, J.E. Leonard, and L. Macindoe

Bushfire CRC

May 2006

Please address all enquiries to:

Bushfire CRC
Level 5,
340 Albert Street
East Melbourne, Victoria 3002, Australia

Distribution List

Bushfire CRC	1
P.A. Bowditch	1
J.E. Leonard	1
A.J. Sargeant	1
L. Macindoe	1
Registry (original)	

Contents

Window and Glazing Exposure to Laboratory-Simulated Bushfires

1. Executive Summary

Windows and glazing systems are prone to damage and failure when exposed to the radiation and temperature effects that a bushfire presents.

Through the Bushfire CRC, the CSIRO Bushfire Research Laboratory at Highett, Victoria, carried out an experimental project in which glazing was subjected to simulated bushfire exposure.

This project aims to provide further information to enable better-informed decisions about glazing design and selection in bushfire-prone areas.

2. Background

One of the main failure modes of buildings is the propagation of fires from burning embers. Window failure gives rise to a point of entry for these embers, allowing for the potential propagation of fires within the building envelope on curtains, soft furnishings, carpets etc. Should these develop or spread, then building loss is almost certain.

2.1 Parameters determining window design, according to AS 3959

AS 3959 *Construction of Buildings in Bushfire-Prone Areas* [1] aims to address many factors effecting building performance under bushfire exposures. Glazing types are chosen according to the risk of failure due to surrounding fuels and topography.

The parameters in AS 3959 that determine the specification of glazing/windows in bushfire-prone areas were used as the basis for experimentation.

2.1.1 Level of construction

The first key factor determining the design of building elements in bushfire-prone areas is the level of construction required.

In the Standard, three levels of construction are defined, which are used to determined as a function of vegetation type, terrain slope and distance from vegetation of the existing/ proposed building, see (AS 3959, Table 2.1), and are based on the level of bushfire risk, i.e. low, medium, high or extreme (see AS 3959, C3.2).

2.1.2 Screening

The Standard states that screening shall be used on all openable windows. Screening aperture size shall not exceed 1.8 mm (see AS 3959, C3.6.1).

Screens may be corrosion-resistant steel, bronze or aluminium. Except in Levels 2 and 3 construction, aluminium is not to be used.

2.1.3 Glazing type

Glazing type for Level 1 construction is not stipulated. For L2 and 3, the Standard states that leadlight windows must be covered with a non-combustible shutter or be made of toughened glass. Toughened glass is stipulated for use in Level 3 construction.

2.1.4 Frame type

Timber used in Levels 2 and 3 must be fire-retardant treated timber except where protected by non-combustible shutters.

2.2 Parameters determining window design, as considered by this project

The intent of the project work was to investigate the common design parameters found in conventional building systems and determine their influence on performance under bushfire exposure conditions. The key variables are:
- Glass type
- Glass treatment
- Glass thickness
- Frame material
- Frame design
- Multi-glazed elements

2.2.1 Windows

2.2.1.1 Glazing type. Glass types employed were toughened, (annealed) plain and laminated. Thicknesses and types of glazing readily available for experimentation are listed in Table 1, with those highlighted being used in experimentation. All glazing used in testing was supplied through a local supplier (see Appendix A).

Table 1. Common glazing available from suppliers

Glass type	**Thickness (mm)**								
Annealed	3	4	5	6	8	10	12	15	19
Laminated			5.38	6.38	10.38	12.38			
Toughened		4	5	6	8	10	12	15	19

The gas-fired radiant panel array (GFRPA) used to supply the radiation load on a specimen has a surface area of 1500 × 1500 mm. As a result, it was decided to adopt a glass dimension that was within this area so as to impose an even radiation exposure across the glass, without creating thermal stress loading across specimens by creating shadowing from uneven radiation exposures.

Glass of 900 × 900 mm was utilised for generic CRC tests as it was within the radiant panel area and thus would not be subject to shading on its outer edges. The cross-sectional dimensions were chosen as they are multiples of 300, which is the basis for most building material sizes.

Other glazing areas varied depending on the framing employed by suppliers, but the overall window dimensions were within that of the GFRPA.

2.2.1.2 Window assembly.

Specimens provided by manufacturers were tested as supplied. All windows made 'in-house' were constructed to hold 900 × 900 mm glazing and were called CRC. Generic CRC frames for timber and aluminium are shown in Figures 1–3.

CRC aluminium window frames were constructed by a manufacturer with glazing and beading being installed on-site. Frames were screwed together with a rubber 'C' shaped extrusion holding the glazing in place within the frame.

CRC timber windows were also manufactured in-house by on-site carpenters. A generic frame cross-section was made, after consultation with our qualified carpenter. Frames consisted of a Mountain Ash main section of frame 35 mm deep by 45 mm high. Machined into this was a 10 mm high by 15 mm deep rebate into which the glass could be placed and a Tasmanian Oak bead nailed in to position with 1.25 mm bright steel brads to hold the glass inside the rebate. Timber species identified here were the names given by suppliers.

Silicone sealant was not used in the window manufacture as the timber beading would hold the glazing in position and the windows were not to be constructed to have a service life.

These dimensions may not reflect the design theory used directly by window manufacturers, but supplied a means of uniformity throughout testing.

Glazing was used as supplied and defects such as 'scalloping' of glass edges was noticed on some pieces of glass but was ignored. The reason being that in normal window manufacturing processes that glazing would not be discriminated against because of this potential flaws. Each piece of glazing was selected on the next piece available principle.

More information on window componentry and assembly as supplied by manufacturers can be found in Appendix B. All windows from manufacturers were tested as supplied or as modified by the manufacturer.

There were neither fire retardant treatments of the timbers used nor any retardant coatings. Silicones were not used in assembly, except where specified in exposure and exposure results.

The design of generic windows used in testing does not include any of the structural loading, glazing selection or installation methods as specified in AS 1288–1994 [12], AS 2047–1999 [13] and AS 4055–1992 [14].

Figure 1. Timber frame (with glazing) – generic CRC.

Figure 2. Aluminium frame (with glazing) – generic CRC.

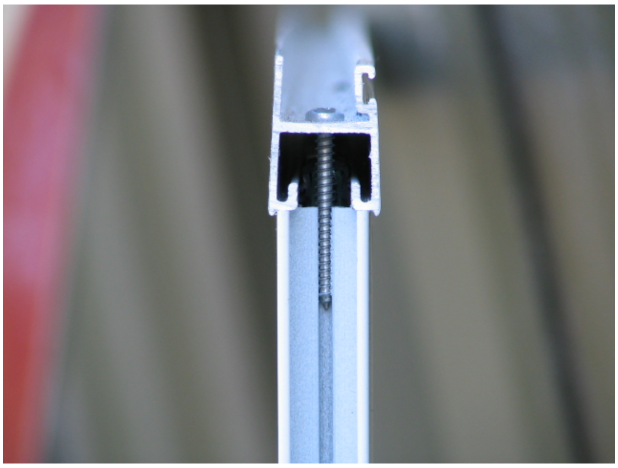

Figure 3. Aluminium frame (profile) – generic CRC.

3. Experimental Apparatus

3.1 An overview

The test apparatus developed for this research was constructed at the CSIRO Bushfire Research Laboratory to simulate the exposure of specimens to bushfire conditions. The system is computer controlled via a feedback loop that provides the means for an operator to predetermine a radiation exposure profile. The following is an overview of the test apparatus, which consists of five main components, viz.:

1. GFRPA.
2. Specimen mounting apparatus.
3. Radiation exposures
4. Computer control.
5. Data acquisition.
6. Laboratory.

3.2 Gas-fired radiant panel array

The GFRPA is 1500 × 1500 mm, and can comfortably expose materials at radiation levels <60 kW/m^2. The maximum limit is difficult to determine as the size of a specimen and its extreme closeness to the panel can create many varied conditions at small distances. This becomes more of a problem with turbulent convective airflow at close range, generated by both the radiant panel and the heated or burning specimens. Figure 4 shows the test apparatus with the radiant panel in the background.

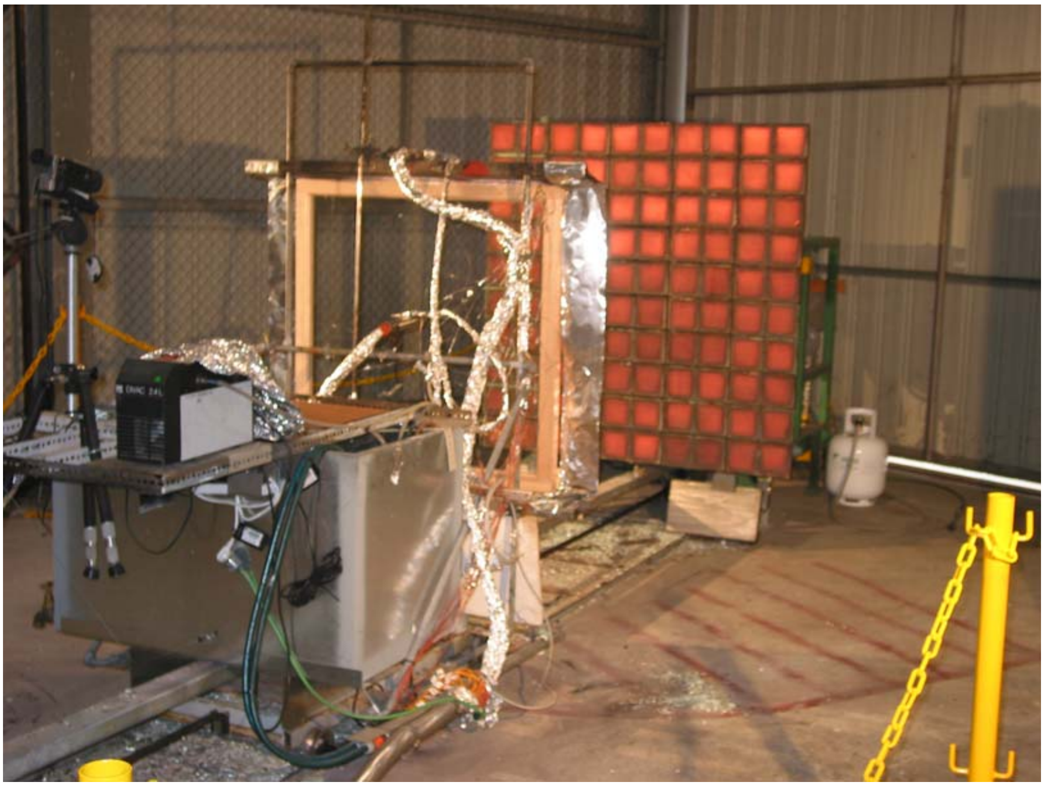

Figure 4. Test apparatus.

The gas used was LPG, which was stored in two 200 L cylinders that, for safety purposes, were stored external to the laboratory (see Figure 5)..

During the exposures, the panel operates at its maximum radiation output, as this is not variable. Radiation exposure to specimens is varied by altering its distance from the panel.

The GFRPA is auto-ignited and a flame rod measures the presence of flaming on ignition. If there is no continuous flaming, the system automatically shuts down and must be reset. This prevents unburnt gas from leaking into the laboratory and creating OHS&E issues.

Figure 5. Gas supply cylinders.

A safe area is designated around the test apparatus with a maximum exposure of 1–2 kW/m^2, being below the pain threshold for bare shin and well below the auto-ignition level of common clothing.

3.3 Specimen mounting apparatus

Specimens were mounted on stainless steel brackets fixed to a water-cooled frame. The brackets were made of a profile as shown in Figure 6. The basis of the bracket design was to accommodate initial tests on glazing without a frame. The brackets were folded into a ‘Z’ shape and were positioned so that their natural spring allowed for the holding of specimens without placing undue loading on the top and bottom surfaces. The brackets were lined with a thin film (approximately 2 mm thick) of Elastosil M4470 high-temperature silicone to enable positive grip of glazing during testing, and to minimise heat transfer from the steel bracket to the edges of the glass.

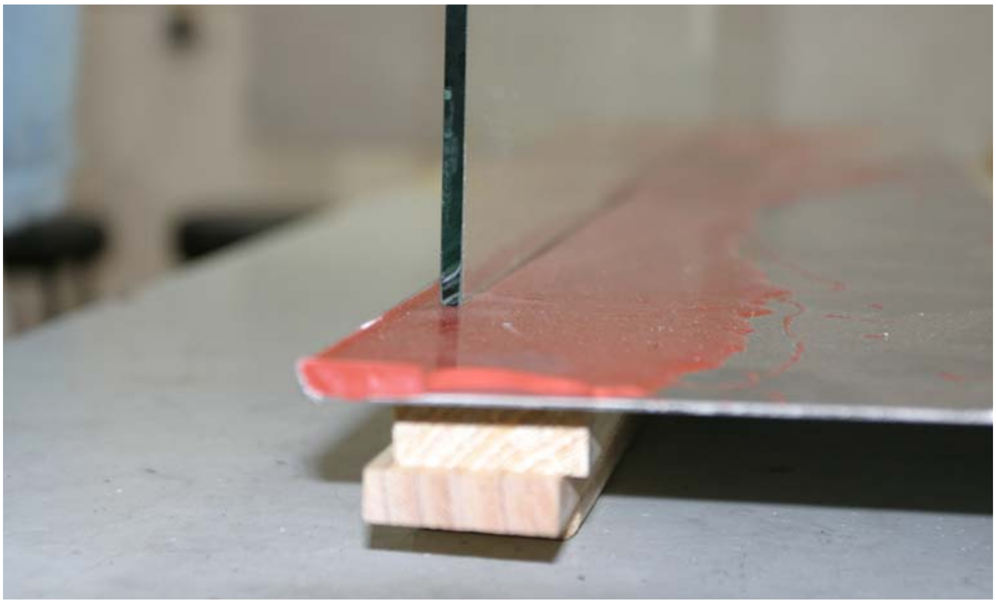

Figure 6. Specimen mounting profile –with Elastosil and glass in-situ.

When framed windows were tested, the brackets were screwed into the window frames to hold them in. Screwing the frames to the brackets appeared to have no detrimental effect on the end results.

The specimen mounting apparatus was on a wheeled trolley that sat on 'rail' track, enabling accuracy of movement in a direction parallel to the radiant panel.

The area underneath the specimen was covered with kaoboard (ceramic fibreboard), which resists high temperatures and does not ignite. The main purpose of this board was to stop convective air currents from passing under the specimen and heating the back face of the glazing elements as there are no sources of high temperature air with a structure during a bushfire event.

A water reservoir was mounted on the trolley to supply water to cool the trolley frame and all onboard radiometers.

3.4 Radiation exposures

Exposure comparisons with experimentation by others

It was deemed important to see the effect that the change in radiation exposure has on glass performance. The characteristics of a radiation versus time exposure recorded were:

- Peak radiation exposure.
- Rate at which peak exposure was attained.
- Maximum time of peak and overall specimen exposure.

The maximum radiation to which a specimen was exposed was decided pre-test. Whether it is from feedback from previous tests, a pass in one test could lead to subsequent testing at a higher radiation level, or by using radiation levels which were considered as critical exposure levels for the particular glass type.

The bushfire exposure simulation to which the test specimens were exposed was a different approach to that used by other researchers. Harada *et al*. [2] and Mowrer [3] used radiant panels in their experimentation.

Cohen and Wilson [4] used a gas-fired burner that supplied mostly a convective effect. McArthur [5] also used a mostly convective source by using a furnace.

Compartment fires were used with windows mounted in a wall by *Shields et al*. [6] and Pagni and Joshi [7]. The heat/radiation sources in these experiments were supplied by liquid pool fires.

In the CRC experimentation, a hybrid of the combined approaches was employed. A radiant panel was used to supply radiation and convective heat, and the distance from this panel was the control used to vary the radiation load on specimens as the radiant panel was operated at a constant output. Both the radiation and the convective heat incident on the windows was assessed the this experimental program. The level of convective heat loss and heat or heat gain will vary greatly in different real bushfire conditions this component of thermal impact is has little discussion in scientific literature.

AS 3959 is currently under review, with much elaboration on the 1999 version and related revisions.

This document does not comment on the current drafts of the Standard, however it does take into consideration developments leading to the Standard's next version. In particular, radiation levels of 12.5, 19, 29, 40 and >40 kW/m^2 are considered in reporting data from experiments. These are likely to be the thresholds that define the bounds of bushfire attack in the Standard's new form.

The testing carried out on the glazing had a main objective of subjecting a glazing system to a radiation exposure which would be indicative of that from a bushfire. As a result, the nature of this testing deviates from fire test methods as prescribed in AS 1530.4–1997.

3.5 Computer control

Accurate feedback of a specimen's location during its travel during testing was achieved by attaching a draw wire linear displacement transducer to the specimen trolley. The control software is programmed with series of 'steps' created to move the specimen incrementally in position control mode. These steps correspond to a known radiation level, as predetermined by profiling the radiation from the GFRPA at any given point along a specimen's travel.

The computer control and logging hardware can be seen in Figure 7. The automation of this system creates a high degree of repeatability of radiation exposures.

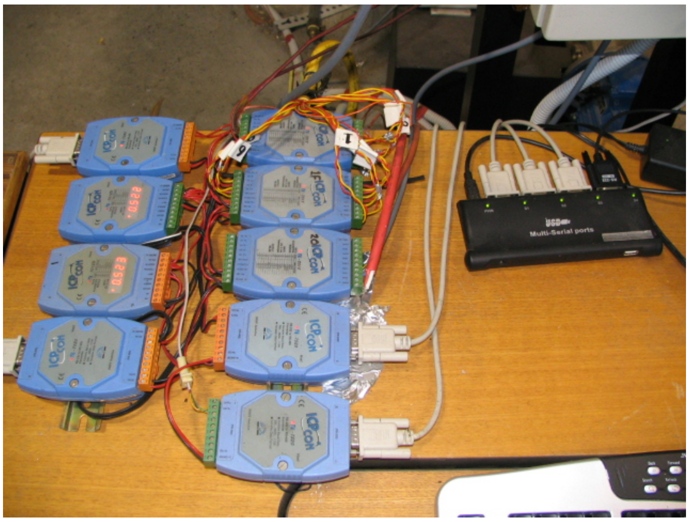

Figure 7. Computer control instrumentation.

3.6 Data Acquisition

Temperature and radiation were the two key measurements during this testing. In addition, atmospheric conditions in the laboratory were constantly measured during testing.

All voltage inputs from measurement devices were converted in real-time to engineering units by the computer software for ‘live’ onscreen display and data collection (see Figure 8). The data was automatically stored in a spreadsheet which allowed ease of graphing and reporting on results.

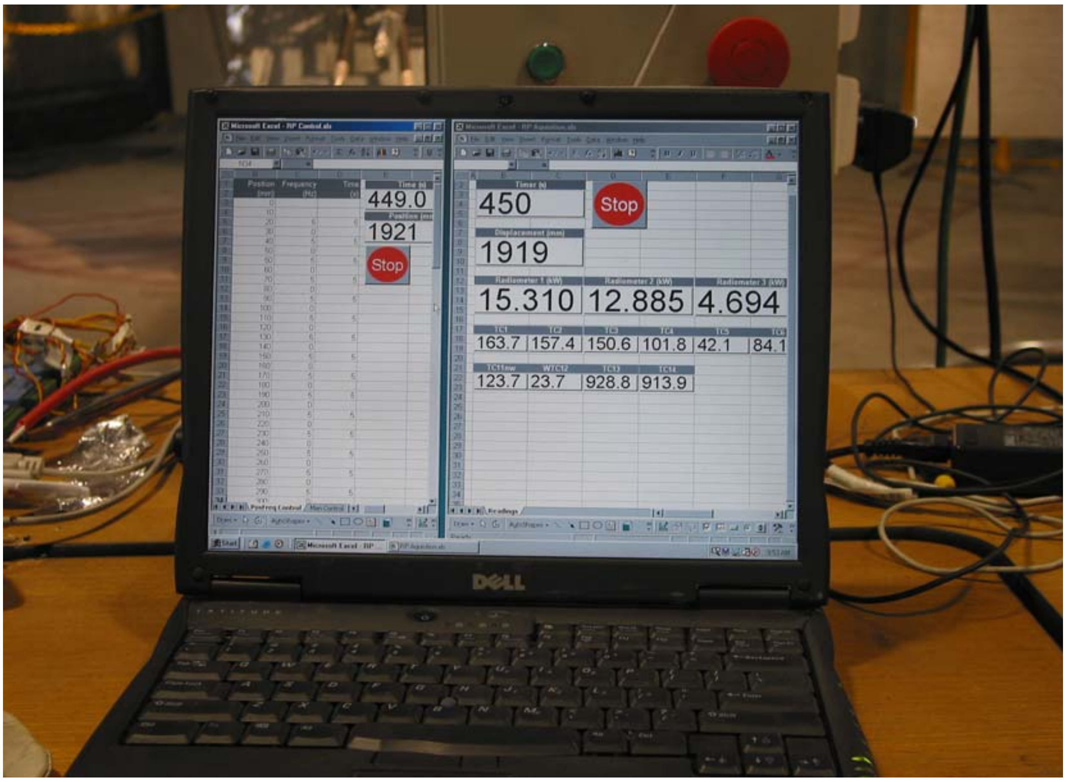

Figure 8. Data acquisition screen

3.7 The laboratory

The laboratory used is a large steel storage shed that accommodates the distance required for specimen travel and provides a safe working space around the test rig. The shed, with its 7 m ceiling height, has the advantage of a large air volume, which helped regulate laboratory air temperatures whilst the GFRPA was operating. This ceiling height also allowed more room for the hot gas layer that evolves during combustion processes. Controlled air supply and hot air layer release allowed a constant supply of fresh air around the apparatus while maintaining air flow rates around the rig below 1 m/s.

3.8 Audiovisual

All tests were digitally video recorded. The video camera was mounted on the rear of the specimen test rig, and thus travelled forwards and backwards with the specimen, keeping its focus on the glazing. The audio was also recorded and was useful in supplying information on aspects of the exposure, e.g. glass cracking.

Digital still cameras were also used to document various stages of the tests.

4. Specimen Instrumentation and Pre-test Preparation

4.1 Temperature measurement of specimens

‘K’-type 1.5 mm Inconnel sheathed thermocouples with unearthed tips were used to measure all temperatures, see Figure 9. These thermocouples have a range of 0–1200°C.

Front and back face temperatures of the glazing were measured in two positions along the centreline of a specimen approximately 150 mm in from the left and right edges of the specimen. This enabled the collection of comparative data on heat transfer through the specimen.

Aspirated thermocouples were located above and below the test specimens at the locations where the upper and lower radiometers were placed.

Aspirated thermocouples were used to measure the convective component of the air surrounding the specimen. K-type thermocouples were placed in a ceramic tube and were spaced from the inner surfaces of the tubes. Air was drawn through the tubes by a vacuum pump past the tip of the shielded thermocouples. The comparison of aspirated thermocouple temperatures and that of unshielded thermocouples, placed at the location of each radiometer, allowed comparison between the radiative and convective components of the heat exposure.

Thermocouples were placed at each radiometer location. Water return temperatures to radiometers were measured to ensure that they were being cooled sufficiently. Radiometers lose their linearity and can be easily damaged if not sufficiently water cooled.

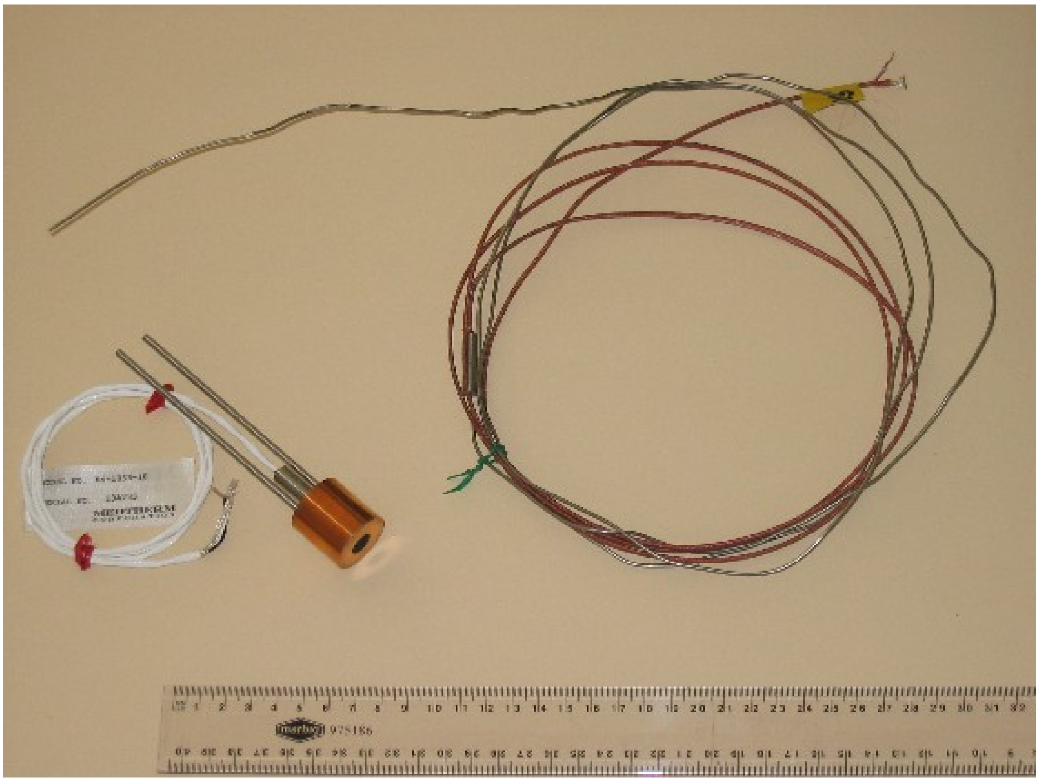

Figure 9. Radiometer and thermocouple.

Thermocouples are factory calibrated and the responses of those used were checked against new ones.

4.2 Radiation measurement of specimens

Radiation was measured using water-cooled Schmidt Boelter radiometers with a sensing range of 0–100 kW/m^2, see Figure 9. Radiometers were factory calibrated and their response was linear, except when used beyond their operating range. Their responses were checked periodically against new radiometers and against an in-house reference radiometer to ensure their linearity.

Radiometers were placed above and below each test specimen, facing the radiant panel. The feedback from the radiometers was used to determine the location of each specimen in relation to the radiant panel to give the desired radiation loading on the specimen during a test.

A radiometer was also placed 25 mm behind the glass in the centre of the specimen facing the radiant panel. This measured the radiation passing through the specimen and gave an indication of the attenuation of radiation incident on the glass.

4.3 Specimen Preparation

CRC window frames on assembly were stored in a shaded area in the test laboratory and were subject to normal atmospheric conditions of the day. There was no conditioning of specimens.

Glazing had all felt tip pen and manufacturers identification stickers removed. Gum residue from stickers was removed with methylated spirits and then window cleaned with a proprietary window cleaner.

Moisture content of timber frames was subject to its stored environment. All CRC timber frames were made in two batches and their moisture contents were measured at random to ensure they were within the specifications of AS 2047-99 [13], which states that at time of manufacture and delivery assemblies must not be less than 10% and not greater than 15% moisture content. Mountain Ash used in the frames has a density of approximately 620kW/m2 and in the unconditioned environment its moisture content did not vary much. Specimens measured averaged 13.6% thus within specification.

4.4 Radiant panel and apparatus calibration

4.4.1 Radiant panel profiling

Thermocouples mounted on the face of the radiant panel were used to measure the panel surface temperature. On reaching a steady state, typically at around 930°C, the panel was ready for use.

To calibrate the test apparatus, the radiant heat flux levels at given distances were measured prior to test to determine specimen position relative to the radiant panel.

Three approaches were used to observe the characterisation of radiation versus displacement from the panel.

A standard approach adopted in fire science is to mount a radiometer(s) in a non-flammable board of a material such as calcium silica (often termed calsil board). This simulates the presence of a specimen so some radiative and convective components are measured by the total flux meter in use.

Another technique that we adopted as a quick check the radiation distance profile, was to place radiometers centrally above and below where the specimen would be, and in the centre of the proposed specimen location. All radiometers faced the radiant panel in line with the proposed glazing test face. This method was used as a quick daily check to determine that all radiometry and temperature systems were operating correctly.

A third method was considered in our experimentation and was deemed to be a more realistic approach. A 900 × 900 mm piece of 6 mm annealed glass was placed in the test rig. Radiometers were in the same positions as per the previous approach, with the central radiometer being accommodated by a 25 mm diameter hole that was drilled in the glass. The data from this was used to determine the radiation level at given locations for daily tests. Using glass as the dummy specimen gave a much more accurate correlation between radiometers 1-3 compared to using other opaque materials such as calcium silicate board or kaoboard.

Figure 10 shows the location of thermocouples and radiometers used on and around the test specimens.

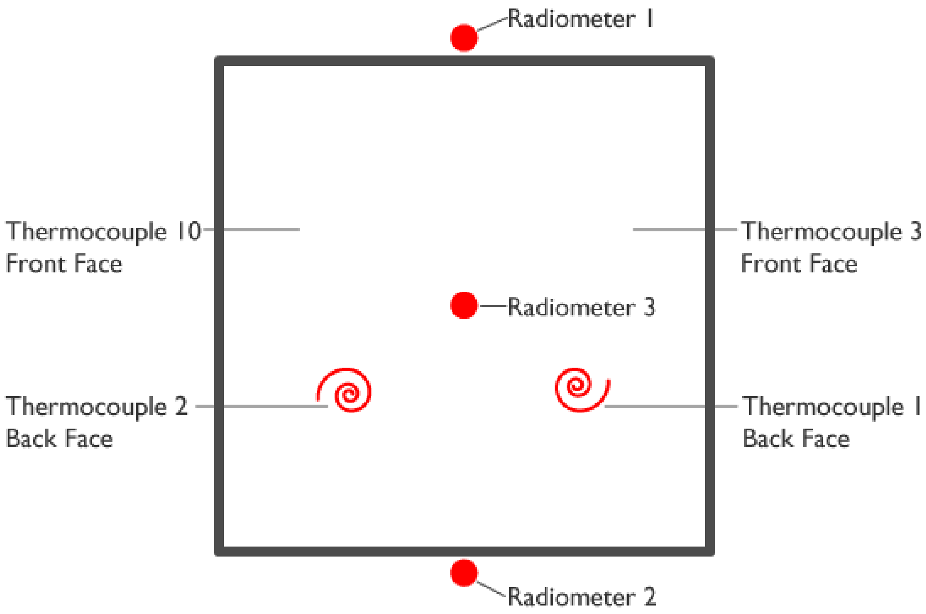

Figure 10. Thermocouple and radiometer locations on test specimen.

Figure 11 shows the data from all three methods used for radiation characterisation. This outlines some interesting results. All radiometer responses for when comparing radiations profiling with glass in place diverge as the radiation level increases.

The three highest curves are using calcium silica board which have higher radiation readings than for the other methods. Calsil board , 30 mm thick was used and on heating it holds more heat within the material as opposed to glass which allows for some radiation transmission through the glass. This can also be seen in Figure 11 by the higher starting radiation measured at a displacement of 3800 mm as opposed to the other methods. The gradual heating of the calcil board creates convection currents which give all radiometers a higher convective component in measurement. Also as the calsil board gets closer to the panel it changes colour from white through tan to brown. This then has the effect of changing the conductive and reflective qualities of the board's face. The darker the colour of the board the more radiation it will absorb creating greater convective radiation and then at close proximities the board then creates a feedback system with the panel, both feeding from each other and this can be seen in the deviation of the radiations at set distances in Figure 11. The results for calsil board deviate markedly from air and glass in place radiations.

When using glass as a calibration surface the central radiometer output mapped very consistently whether the glass was in place or not. This allows the second method without a glazing element in place being a suitable instrument check.

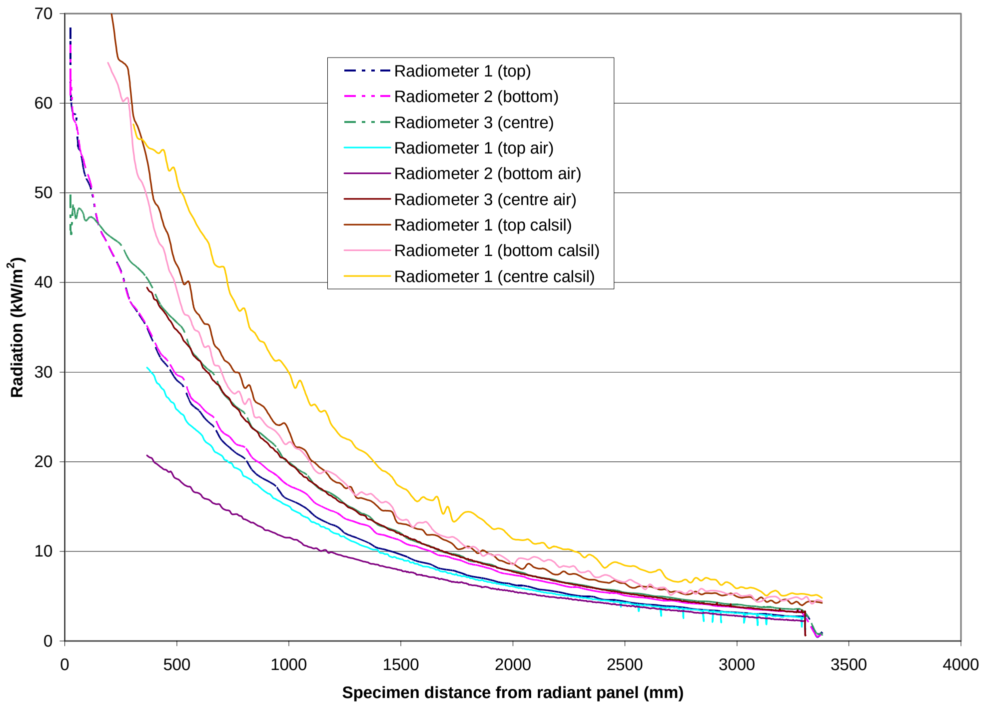

Figure 11. Radiation versus specimen distance from panel – in glass, calsil and in air.

Initially it was thought that radiometer 1 (top) would be the best feedback radiometer during testing to estimate the front face radiation of the glass, however experiments revealed that the flaming and convection from burning specimens greatly effects this radiometers output.

Air calibration of the central radiometer and acknowledgement of test rig displacement was used as feedbacks to check measurements.. Radiometer 2 (bottom) and its offset per Figure 11 were used as feedback during tests to estimate radiation load on the centre of the front of the glass. The effects of flaming of specimens greatly affects the perceived radiation exposure of a window so these two techniques were considered the best options for a non flaming condition.

In addition to the previous technique a profile across the specimen area was carried out giving a view of the radiation profiles a specimen would receive at three distances from the panel. In this method the calsil board was employed as previously. Figure 12 shows measured results at the distances 1, 2 and 3 metres from the panel. This serves a double purpose checking that their is not significant variation across the panel in radiation whilst also giving data that could be used for data correction when observing radiation and temperature profiles across surfaces.

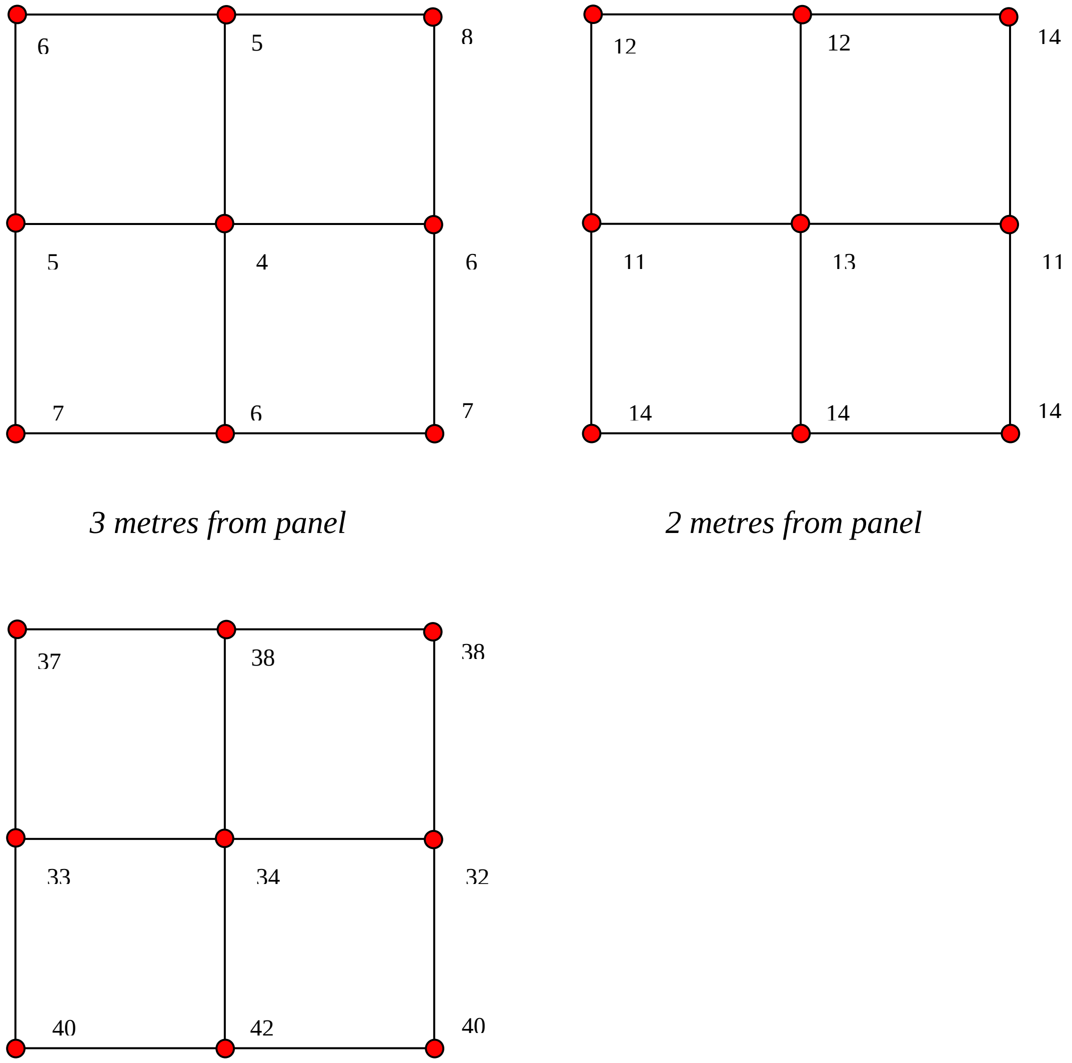

3 metres from panel

2 metres from panel

1 metre from panel

Figure 12. Radiation profiling across specimen area

4.4.2 Instrument check

The displacement transducer used for position feedback was checked for linearity by moving the test rig a set distance and measuring its displacement with a tape measure.

Radiometers were checked by observing their feedback responses at predetermined locations and cross-referencing with data obtained on previous radiation profile runs where radiation feedback was observed without a specimen in place.

Thermocouples were periodically checked to verify that they were responding to known heat sources.

4.5 Test apparatus radiation characterisation

To predetermining the radiation profiles that would be used for bushfire simulation, it was important to characterise the radiation versus displacement from the radiant panel.

Firstly, the radiant panel was characterised by measuring radiation at set locations across the panel at varying distances from the panel. This gave indicative output of the radiant panel across its face. Adjustment of gas flow, by a gas fitter, to each of the panel's elements then allowed the radiant panel to be tuned to obtain the most consistent radiation across its face (refer to figure 11).

To establish the radiation received by a glazing unit at any given distance from the panel, a profile of radiation of versus displacement was measured over the full length of travel of the test rig.

In normal testing, it was decided to have a radiometer above and below the glazing, and one 25 mm behind the glazing in the centre to measure back face radiation.
In characterising the test rig, it was decided that the best approach was to measure the radiation that would be imposed at the centre of the glazing. A 6 mm thick annealed glass panel 900 × 900 mm was placed in the test rig. This glass panel had a 25 mm hole in its centre into which was placed the radiometer normally used for back face radiation measurement.

This test setup was chosen to be more indicative of the radiation received during testing on glass. Normally in laboratory experimentation, cement sheet or calcium silica board is used instead of glass. This does not have the same radiation responses to heating as glass. Also, glass doesn't off-gas and there would be no issues of moisture egress on heating or the potential for any flaming.

The test apparatus was moved toward and away from the radiant panel, and it was the feedback from the central radiometer that was used for the basis of future test profiles.

4.6 Test radiation profiles

Initial test radiation profiles were performed at a simplified constant test rig speed to assess specimen and rig response. The full speed of a 240 V AC motor is 60 Hz. The motor speed rates chosen for initial testing were 10, 30 and 60 Hz. These equate to a linear speed of the rig of 0.01, 0.03 and 0.07 m/s, respectively. This meant that only one speed could be used during the test, and distance in relation to the radiant panel was measured as a function of distance over a given time (see Figure 13).

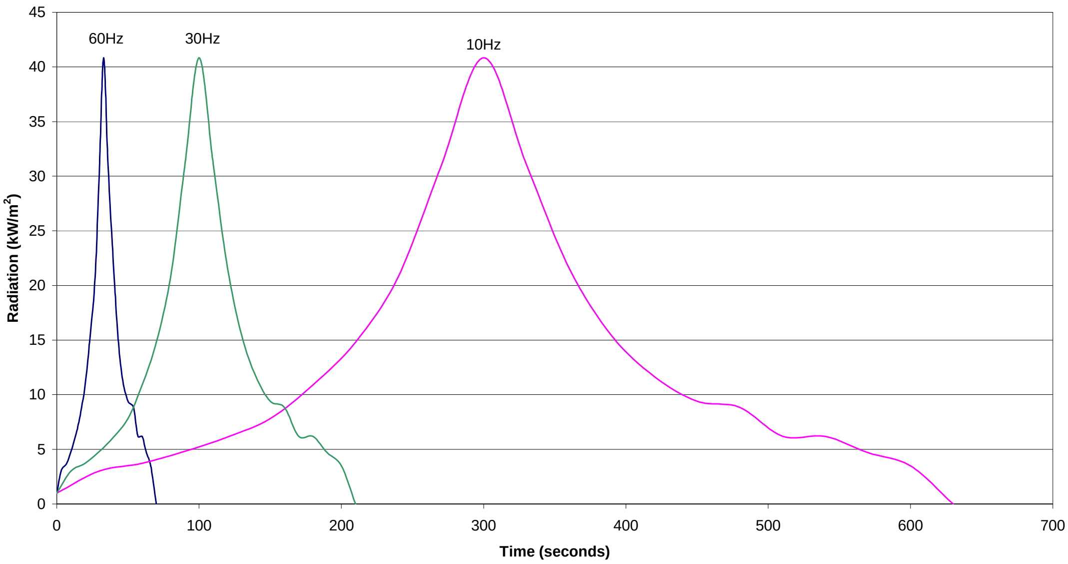

Figure 13. Frequency controlled radiation profiles versus time

We endeavoured to use various frequencies over specified time sequences to create a radiation exposure curve, but this proved difficult. Software proportional, integral and derivative control was investigated with in-house purpose-built software, but this proved inadequate as over- and undershoot of the test rig's location created issues with the repeatability of results.

With test apparatus and software modification it became possible to use a combination of displacement and motor speed to develop the fast and slow bushfire profiles used for the majority of testing. Incremental steps of displacement movement at predetermined speeds. Obtaining the displacement transducer allowed accurate distance movement that was repeatable. The radiation profiles simulating bushfire exposures are shown in Figures 13 and 14.

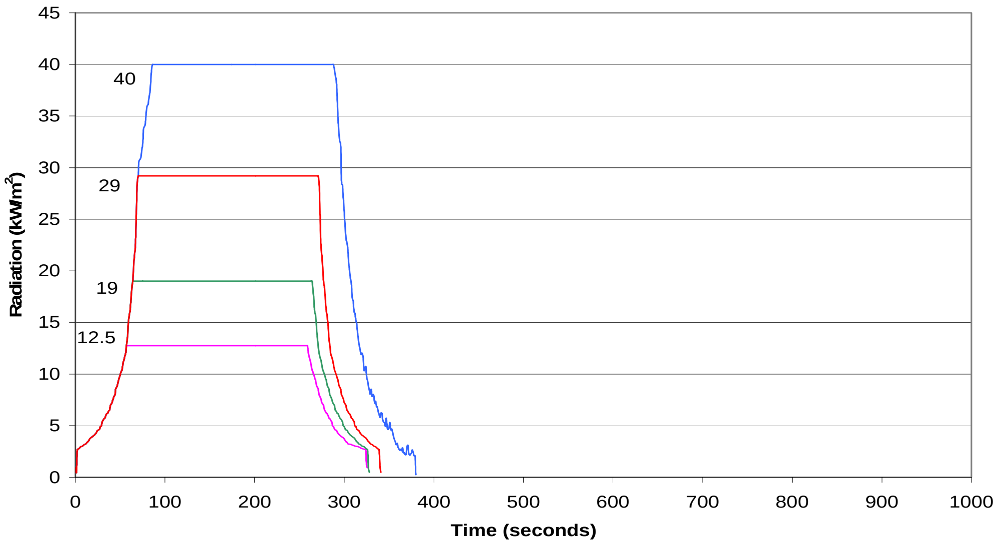

Figure 13. Fast profile radiation exposure – radiation versus time.

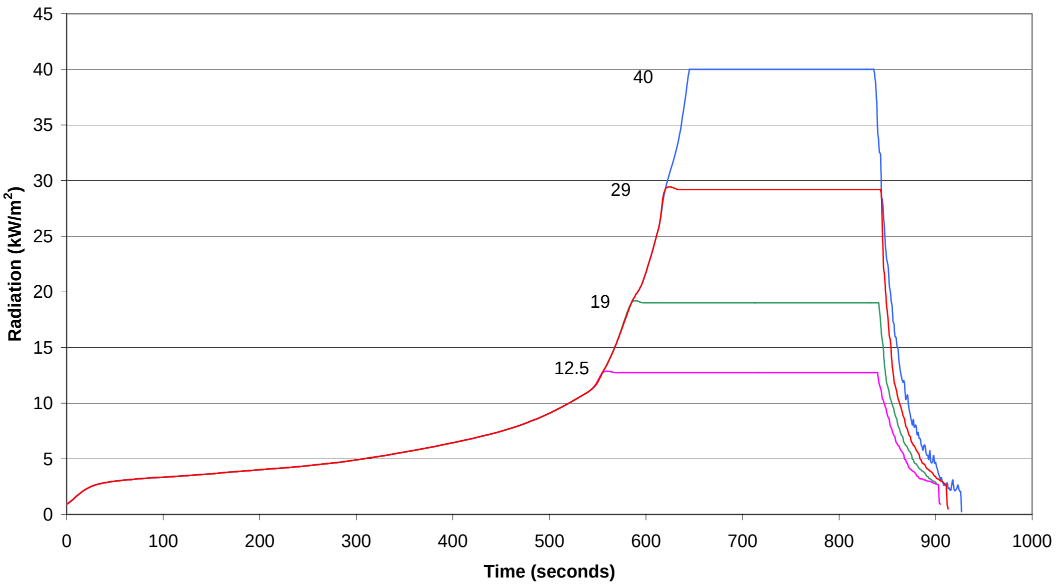

Figure 14. Slow profile radiation exposure – radiation versus time.

It was found during testing that the slow profile best represented a bushfire exposure of slow build up, and this profile provided the greatest incident heat load on specimens. The inclusion of a wait period in the profile allowed for the simulation of bushfire approach, immersion and passing.

The slow heating of a specimen allowed more time for the glass and glazing elements to reach critical levels that affect their performance under simulated bushfire exposures. Elements such as seals or paints in particular can reach points where they off-gas enough volatiles thatwill ignite under piloted ignition conditions.

As an example, specimen Trend 14 used a fast profile and, on reaching the point of closest proximity to the panel the glass temperature reached 81°C, in comparison to Trend 12 using the slow profile the glass temperature reached 235°C. To highlight the differences further, Trend 12 ignited and Trend 14 did not.

4.7 Laboratory conditions

Due to the nature of this work and the localised weather pattern that the radiant panel creates in the laboratory, there was no attempt to control ambient temperature and humidity. Instead, the laboratory temperature and relative humidity at a set distance from the panel were constantly logged during testing.

Two of the large roller doors to the laboratory were partially opened during testing to allow egress of the hot gas layer at the ceiling level, and also to reduce the effect of external wind on laboratory conditions, and to also maintain airflow rates in the laboratory to approximately 1 m/s. This is a figure quoted for laboratory fire tests in AS 1530 [8]. However, convective currents in the upward direction created by the radiant panel may have negated this figure in localised areas around the test specimen and apparatus during a test.

More information on laboratory condition measurements is given in Appendix D.

5. Experimental Procedure

5.1 Prior to test start

Prior to test start, specimens were placed on the test rig and all radiometers and thermocouples were positioned.

A piece of cement sheet was fixed to a trolley and was wheeled into position so that it shielded the test specimen from radiation whilst the radiant panel was in operation.

The radiant panel was prewarmed prior to each test and its readiness was confirmed on stability of the panel temperature, as read from a thermocouple embedded in the panel face. This temperature was typically around 950°C. In earlier tests, a Nomex blanket was hung over the specimen, but this proved inadequate if quick turn around of tests was required. The cement sheet also created a radiation protective safe working area for installing new specimens and protective the specimen installer while the panel was operating. This allowed for quick turn around of experiments without uneccesarily shutting the panel down.

Air profiling was performed as per 4.4.3 to establish correct radiation feedback.

The radiation test profilewas selected and, on completion of radiant panel warm up, data logging was commenced and specimen testing started on the removal of the protective shield.

All personnel were kitted with the appropriate personal protective equipment, and visitors were given a safety briefing and kept a safe distance from the apparatus to avoid radiation exposure greater than 2 kW/m^2.

5.2 Testing

The radiation profile was commenced and the shadowing of the specimen cement sheet panel was removed to expose the specimen.

During the specimen's travel, observations were made as to when specimens were off - gassing, cracking, flaming and breaking.

The off-gassing of volatiles from window components during heating were 'piloted' by moving a lighted stick in the region of the volatiles to initiate ignition (see Figure 15). Care was taken to maintain a separation distance of at least 30 mm from the specimen during piloting to avoid direct flame contact with window assembly.

Figure 15. Piloted ignition.

On the breaking or failure of a specimen the test was deemed to have ended, otherwise the specimen continued its radiation profile.

5.3 Modes of failure

An acceptable method of defining the mode of failure of a window system is when the performance of the system is such that it provides a significant escalation in the level of risk of house loss. This could occur due to the window allowing entry of embers and/or flames into the structure, or the flaming of the window system providing a significant additional flame impingement on other elements of the structure, potentially causing them to fail. In most cases a failure is considered where a gap of the high probability of a gap occurs. For example a plain glass window assembly is likely to create a gap when the window first breaks however is some cases the glass cracks but does is not displaced, in this case we consider it as failed as wind conditions in a real bushfire is likely to displace the glass. In some cases where laminated glass or polymer coatings are used it can be argued that the polymer system restrains the cracked glass fragments for some time after first crack occurs. In these cases the time to failure is more subjective as an opening need to be observed and averaged over a number of test runs.

For this investigation the modes of failure considered were:

- Glass cracking (not necessarily glazing integrity breach) (see Figure 16).
- Flaming on the inside of the frame (see Figure 17).
- Glazing breach by shatter and thus glass displacement (see Figure 18).
- Glazing assembly breach by gaps 2 mm or greater opening within the glazing or between glazing and frame.

Figure 16. Glass cracking.

Figure 17. Internal flaming.

Figure 18. Glass shatter.

6. Glazing System Tests – Background Discussion

6.1 Other radiation exposure experiments by comparison

6.1.1 Test apparatus

Much theoretical and experimental research has been done on the breakage of windows using fuel tray fires as heat sources in compartment fires [6,7,9].

McArthur [5] used a gas-fired downdraft vertical furnace to which window assemblies were fixed. Rather than using a bushfire radiation profile as developed as part of this CRC project, he used a time versus temperature curve, as prescribed in AS 1530, Part 4 [8], to simulate the effect of an external building fire on a window.

Cohen and Wilson [4] used a wind tunnel utilising a propane gas burner as a heat source. This experimentation was interesting because the wind tunnel allowed the additional simulation of driving embers (brands) at the windows. This research is of interest in the Bushfire CRC and shall be investigated further as part of future research.

Harada *et al.* [2] used a gas-fired radiant panel, as did Mowrer [3]. The CRC testing used a much larger gas-fired panel of 1500 × 1500 mm and, as a result, could test larger specimens than those reported by other researchers.

In all experimentation, the test sample was in a fixed location and heat sources were either built over time in the case of the crib, furnace and pool fire experiments, or the heat load was constant, as in radiant panel experiments.

The CRC experiments varied by moving the specimen and maintaining a constant radiant panel radiation load. This allowed various bushfire profiles to be employed by changing the rate of movement towards the panel to better simulate the radiant heat flux profiles that would be expected from a bushfire.

Harada *et al*. [2], Mowrer [3], and Cohen and Wilson [4] observed that the thermal fields applied to exterior glass by fires was a better observation of the effects of flaming from bushfires.

6.1.2 Failure modes of interest

The CRC research attempted to understand the mechanisms that cause failure, and concentrated on internal framing and glass crack as the primary failure modes. It was important to note also that the metamorphosis of a window design, as in the Trend series of tests, could effect the outcome of its performance. Frame type and flaming were observed as factors having a major contribution to failure, and this will be discussed further in the conclusions.

Cohen and Wilson [4] were interested in failure (cracking) and also observing openings within the glazing that could allow for ember entry. Others such as Harada *et al*. [2] were interested in glass fall out.

Shields *et al.* [6] observed temperature gradients across glazing, and also reported first cracking and opening of glazing (venting).

Pagni and Joshi [7] related the mechanical breaking stress of glass to heat transfer within the glass.

Mowrer [3], Keski–Rahkonen [9], McArthur [5] and the CRC were interested in first crack failure. This is a good point of failure observation as it is difficult to surmise the events that occur after first crack.

6.1.3 Specimens and their exposure

One of the difficulties is cross-correlating the recorded data. In McArthur [5], for example, data was obtained for glass failure, but this does not directly equate to glass temperature nor does it equate to radiation load. AS 1530.4 uses a time–temperature curve that is followed to create the test environment. Radiation levels are not obtainable as they are not measured, and temperature at such a small interval of 30 seconds is not obtainable with any accuracy as the initial warming of a furnace will vary from furnace to furnace.

In their experiments, Harada *et al*. [2] looked at glass cracking and fall out as a result of radiant heat exposure. Their work on 3mm float glass and 6.8 mm wire glass, exposed glazing to radiation levels of 3–10 kW/m^2.

The radiation levels employed as part of the CRC project were up to 60 kW/m^2 by comparison, which is approaching the point in which flame immersion in a bushfire is imminent. However, there are limitations at levels over 40 kW/m^2, in that the feedback process between radiant panel and test specimen can lead to spurious results, especially if specimens are flaming.

Shields *et al*. [6] used 500 × 500 mm and 900 × 900 mm fuel trays to apply two rates of bulk temperature loading on 6 mm annealed (float) glass.

Using cribs, Cohen and Wilson [4] obtained radiation exposures of 9.3, 13.6 and 17.7 kW/m^2 in tests using 610 × 610 mm annealed and toughened glass.

Pagni and Joshi [7] used 2.4 mm thick 280 × 510 mm annealed glass, with a heat source supplied via 20 mm diameter hexane pool fires of either 300 × 200 mm or 200 × 200 mm.

Mowrer [3] tested annealed glass, toughened, heat-resistant ceramic glass and wind-resistant laminated glass, using a gas-fired radiant panel at heat fluxes of 2–16 kW/m^2.

CRC experimentation observed data from unframed, timber framed and aluminium framed glazing. Glass thicknesses or glazing combinations varied from 4 to 10.38 mm, and heat flux exposures and rates of exposures were varied. Glazing included annealed (plate), toughened (tempered), laminated and double glazed. Radiation exposure limits followed those outlined in AS 3959, but the build up of exposures to simulate bushfire exposures was an ‘in-house’ ideology based on previous work.

One of the things apparent in this reporting of data is that researchers must be very specific in reporting glazing, thickness, type and even supplier. Should this experimentation need to be revisited, all facts should be reported.

Excellent references on research carried out to date are by Babrauskas [10] and Hassani *et al*. [11] where they summarise research carried out and their findings.

7. Experimental Results and Discussion

7.1 General

The test data is reported in Appendix A and has been divided into sections, i.e. unframed, timber framed and aluminium framed.

The data reported in the tables includes peak radiations and temperatures. It is important to note that these peaks are reported for failed specimens at the time of failure. For those specimens that did not fail, the peaks reported are the highest during the experiments.

Failure of specimens was;

- First crack
- Internal flaming
- Shatter

Data presented is divided into glazing types and does not discriminate between slight frame variations during testing. This will be discussed later in this section.

Trend and Canterbury proprietary window experiments and Bekaert film testing are discussed in Appendix B.

7.2 Unframed glazing

7.2.1 General

Initial experiments sought to look at the performance of unframed glazing under various radiation exposures, to attempt to provide background information on the behaviour of glazing under radiation loads.

A total of 23 experiments involving unframed glass were carried out to gather a general understanding of the performance of glazing when not restrained and when not enclosed around its edges.

It was observed during experimentation that specimens bowed under heating, indicating that the outer surface of the glassing element is hotter the inner and the expansion of this outer layer results in the observed deformation. The magnitude of this effect was not measured.

The silicone-filled Z bracket holding the glazing in place top and bottom was installed to apply just enough pressure on the glazing to hold it in place without creating mechanical stress on the top and bottom edges. This proved successful in experiments as glass flexure could be observed with the naked eye yet the glazing stayed within its holding frame. As a result of this low profile fixing, edge shading was reduced to approximately 1 mm. The silicone also greatly reduced the effects of heat transfer from the stainless steel Z bracket to the glass edge.

Results from all unframed tests can be seen in Table A1.

7.2.2 Unframed annealed glass

Annealed glass 4 mm thick was subjected to various radiation profiles as seen in Figure 19. Various fast and slow radiation exposure profiles are shown with different wait periods at peak radiation exposure. Radiation exposures are based on test apparatus speed rates and do not reflect a true bushfire exposure profile.

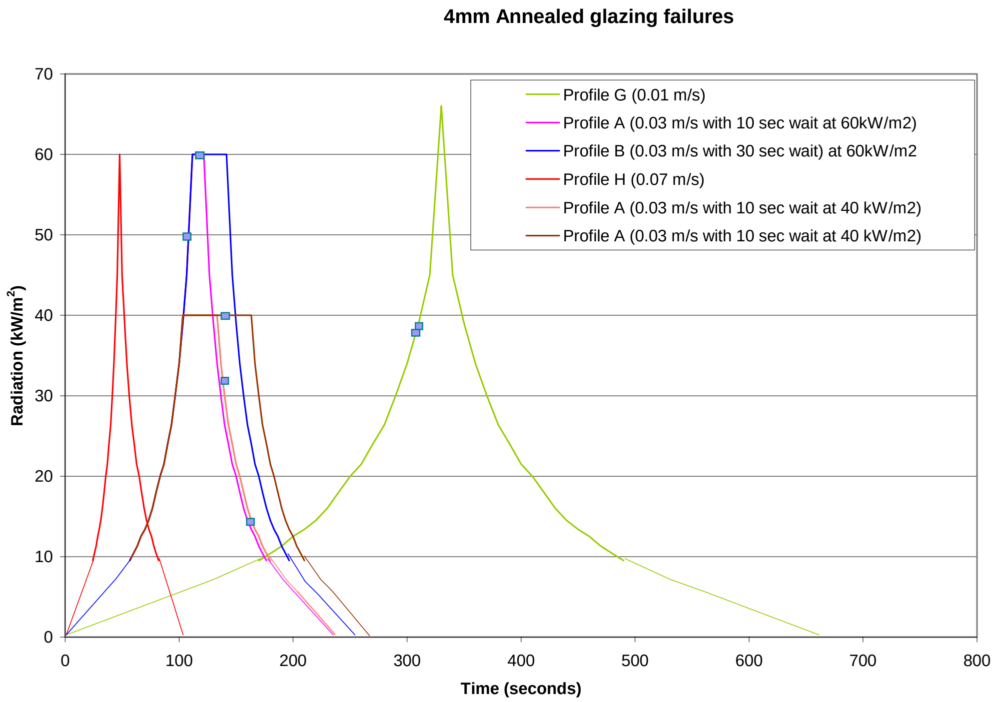

Figure 19 Radiation profiles with.4mm Annealed glazing failures

Figure 19 shows a summary of the range of profiles use, the dots on these curves represent the point of failure for each exposure if a failure occurred, for more detail data refer to appendix A. The faster the radiation profile the less likelihood the specimen will fail. No specimens at the fastest speed of 0.07 m/s failed. This is because their. was insufficient time for thermal transfer of heat into the glass creating the stresses that cause failure and interestingly no thermal shock failure observed.

Specimens following a 0.03 m/s feed rate intending to peak at 60 kW/m^2 failed at 50 and 60 kW/m^2, with an additional specimen failing on the return leg of the profile at 12 kW/m^2.

Specimens following a 0.03 m/s feed rate to 40 kW/m^2 where given wait periods of either 30 or 60 sec with all specimens reaching 40 kW/m^2. Specimen 4PL30D was on a wait of 60 sec and failed at 155sec into the test, a period not long after when the 30 sec wait would have finished. It is likely that had it been on a 30 sec wait as was the other specimens

These results indicate a wide spread of data for annealed unframed glass with failure modes being greatly effected by the speed of testing.

7.2.3 Unframed laminated glass

All laminated glass failed by cracking. When the interlayer broke down under thermal loading, it gave off gaseous vapours. The formation of these gases and their expansion created mechanical stresses that broke the bond between the glass layers, and this stress was transferred to the outer edge of the glass, compounding the effect of thermal load on glass breakage.

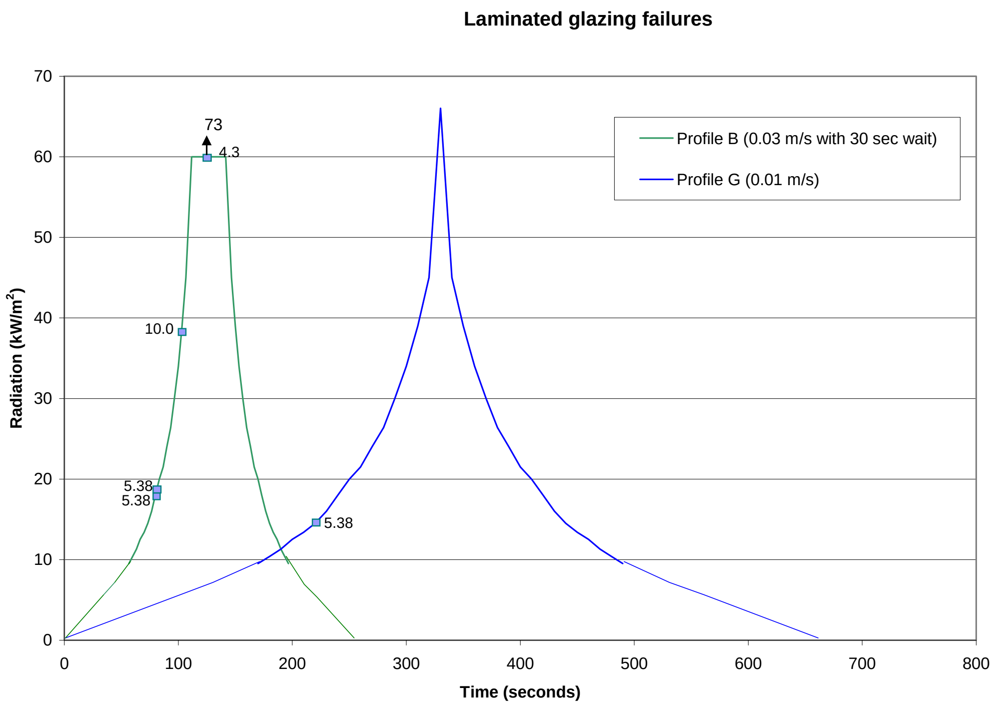

Figure 20 Radiation profiles v. Laminated glazing failures

Two radiation profiles B and G at 0.03 and 0.01 m/s respectively were carried out in this small data set, refer to figure 20, the points on the graph depict different point of failure and are labelled according to thickness. With the data set not being larger it is difficult to draw too many conclusions.

Only one specimen 5LA30A failed at a radiation over 40 kW/m^2 all others failing under this mark.

The specimen 5LA30A that had a a measured failure radiation of 73 kW/m^2 was unusual in that at this location the perceived radiation should be 60 kW/m^2. The additional radiation measured would be from convective radiation from the radiant panel and from the glass. Being the thinnest of glasses tested there was also greater flexure visible by the glass before failure. The extra heat loading on this glass is also visible in the peak front face temperature which was 422 ^{o}C the only other highest was the 10 mm glass which reached 249 ^{o}C. It could be that this test data is an outlier and may need to be ignored but only additional testing would tell.

The 10 mm glass, L10A30W30, failed at 38 kW/m^2 and its thermal thickness and rigidity would have played a role in prolonging its duration of exposure before failure. All other tests failed at 19 kW/m^2 or less.

One specimen L5A30E20 had 20 mm of foil around its edge to observe whether edge effects such as shading would change its failure radiation. It was also hoped that edge sealing would reduce the time to delamination and failure but this appeared to have no effect with failure occuring at 18 kW/m^2.

In summary, it is interesting to note that laminated glass without frame failed sooner that annealed glass.

8.2.4 Toughened glass

.Radiation profiles used in this small data set were G, H and B, see Figure 19.

Specimens T4A10E20 and T4A30E20, which were 4 mm toughened glass, were tested at 10 and 30 Hz, respectively. These specimens also had 20 mm of aluminium tape around their edge to simulate the shading effect that a window frame might impose on the glazing. In these cases, 28 and 29 kW/m^2 was reached without any glazing failure on exposure nor any failure on cool down.

Specimen 5T30A was the only specimen that failed through cracking at 68 kW/m^2 well over the primary peak level of interest in this investigation 40 kW/m^2.

8.3 Framed glazing

8.3.1 General

Different types of both aluminium frames and timber frames were exposed at various levels as detailed below..

Aluminium frames were either as supplied by Trend Windows or were made as part of this CRC project (termed generic CRC frames). CRC frames were single pane and were not part of a complete openable or fixed window unit. Trend windows were a combination of fixed, sliding and awning windows with and without timber reveals.

All results for framed glazing failures and their radiation profiles employed are graphically represented in Figure 21.

8.3.2 Timber framing performance

8.3.2.1 Annealed and laminated glass in timber frames.

Results to be considered in further work.

8.3.2.2 Toughened glass in timber frames. As no failures were observed for levels of 12 19 and 29kW/m2 Tests on 4, 5 and 6 mm toughened glass were at <= 40 kW/m^2 .

The most interesting trend in all data is that of the 10 specimens that experience frame flaming 4 did not fail, these having foil covered rebates, see section 8.3.2.4 for further discussion.

At the faster feed rate profiles of E and H, specimens 6TFA40F (6 mm) and 5TSH40 (5 mm) passed 40 kW/m^2 with there being no flaming of their frames. This is to be expected as movement toward and away from radiant heat sources at faster rates gives less chance for frame temperatures to rise increasing the chance of flammability. Critical temperatures for frame ignition cannot be generalised as timber species, frame dimensions and finishes all effect results.

At the slow profile F, all 4 mm toughened glass failed, however it was significant that three out of five experiments failed on cooling down after peak exposure. This is a failure mode worth o further investigation as to the cause and mitigation of this failure during cooling.

Out of 10 tests at profile F, only one 5 mm toughened glass passed 40 kW/m^2.

The effect of frame flaming on glazing failure in these experiments, did not appear to have a direct correlation to pass or failure of the glassing element. Figure 19 shows front and back face temperatures for passes and failures. A linear trend line through the data shows a wide spread of data and that there is no real trend here.

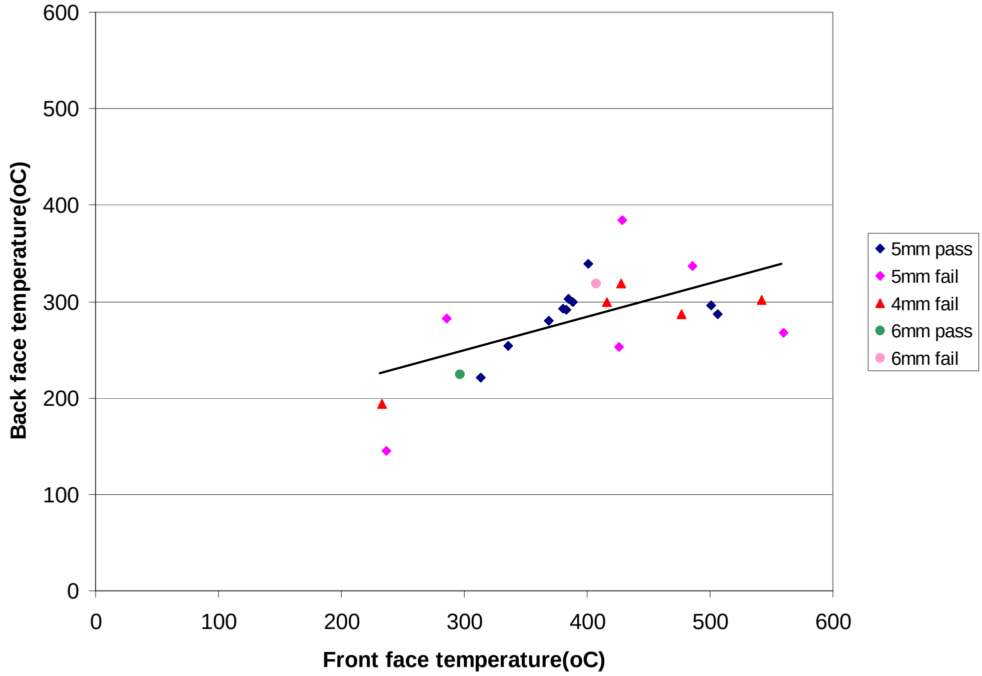

Figure 19. Peak front and back face temperatures of toughened glass.

8.3.2.3 <u>Glass temperature profiles</u>. Keski–Rahkonen [9] theorised that the thermal stresses created between shaded glazing edges and unshaded areas could cause glass breakage. He calculated a temperature differential of 80K (193°C) at maximum stress in soda glass.

To investigate this on timber frames, rebate thermocouples were placed between the glass and the timber frame (Rebate 1) and between the glass and the beading used to hold the glass in place (Rebate 2). A thin layer of ceramic fibre wool was place between the thermocouples and timber surfaces to insulate between the timber and glass to give truer glazing temperatures, minimising heat sink from the timber.

Figure 20 reports the results from window temperatures measured on 6 mm toughened glass in a timber frame which was tested up to 40 kW/m^2.

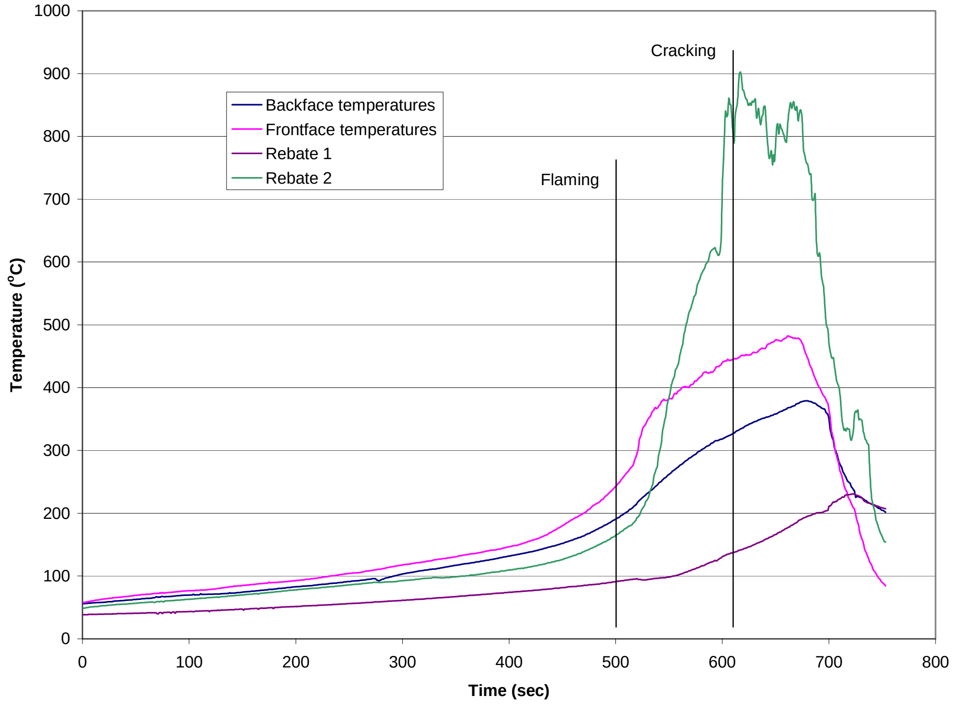

Figure 20. Typical 6 mm glazing temperatures (specimen 6TTFB40S).

Data plotted is the average front face temperature, back face temperature and the two rebate temperatures.

Front face glazing temperatures in this experiment had a differential of approximately 100°C at failure, glass crack, and averaged to 332°C. Back face temperatures at failure averaged 448°C, a differential across both faces of 116°C.

8.3.2.4 Edge effects on timber frames.

Further work to be done , results not conclusive.

8.3.3 Aluminium framing performance

8.3.3.1 Annealed and laminated glass (in Aluminium frames).
Results to be considered on further work.

8.3.3.2 Toughened glass. Two series of experiments were carried out on toughened glass in aluminium frames: Trend window tests (see Appendix B1) and generic CRC frames.

It is important to note that the difference between these two series is that the generic CRC windows were single lights and were framed around the glazing only. There are no reveals, weather stops nor window furniture. Some Trend windows were like this but most were in window units, single or double lights and some had reveals.

Only one specimen (Trend 5) cracked after an exposure at 40 kW/m^2. The majority of specimens passed this exposure, except four (Trend 12, 17, 20 and 21) where seals failed and internal flaming occurred. In these tests, there was insufficient heat from combined flaming and radiation to crack or shatter the glass.

Of the tests that passed the initial exposure of 40 kW/m^2, eight of these failed on cool down all having rubber seals. One in particular (Trend 8) shattered 2.5 hours after radiation exposure. Interestingly all 16 toughened glass windows with silicone seals in place did not fail during cool down.

The 15.38 mm combined annealed and toughened glazing all failed via cracking of the annealed glazing. However the inner toughened glazing did not fail, so although this is a failure of the system is it to be considered a failure. At slow profile E, Trend 11 and 4,the peak radiation on cracking was 11kW/m^2, and at the faster profile F, Trend 7, it was 39 kW/m^2.

8.3.4. Aluminium versus timber frames

It is clear from data gathered that there is a difference between timber and aluminium framed window performance.

With varying section sizes and glazing sizes direct comparison of data may be misleading, but to simplify discussion all aluminium results are pooled together as are timber. Changes in framing section sizes and material type will affect heat transfer between glass and framing.

The additional loading that flaming frames have on glazing performance does seem to affect the potential of failure. With timber frames, 14 flaming frames failed and 4 did not. With aluminium frames, 8 flaming of seals failed and 7 did not. However to for these toughend glass exposures timber frame failures are much for prevalent.

Table 2 summarises the results from all tests and the pass/fail data. By explanation in each column there is an alpha numeric e.g. 16B, this equates to 16 kW/m^2 using radiation profile B. In each row is the ranges of radiations for each profile. This may seem somewhat confusing so to simplify Table 3 indicates the maximum possible exposure at which a specimen passed.

Table 2. Peak radiation loads causing pass or fail for each profile

Glass	**Aluminium**		**Timber**	
	Pass	**Fail**	**Pass**	**Fail**
4 mm annealed	13C	22D	-	12C
4 mm annealed (film)	6F, 6H, 6C, 16D	-	-	6F, 7G
4.38 mm laminated	-	20D	-	20D
5.38 mm laminated	<16B	16B	-	23B
3 mm toughened	23F	40F	-	-
4 mm toughened	+40F, 50B	40F	-	
5 mm toughened	40F	40F	46H, 31F	44F
6 mm toughened	40E	-	40E	40F

Table 3. Peak loads causing pass or fail

Glass	Aluminium		Timber	
	Slow	Fast	slow	Fast
4 mm annealed				19
4 mm annealed (film)				
4.38 mm laminated				20
5.38 mm laminated				23
3 mm toughened				
4 mm toughened			40	
5 mm toughened			+40 no fail	+40 no fail
6 mm toughened				+40 no fail
15.38 mm lam/tough				

Laminated and annealed glass failed at levels below 20 kW/m^2 for the sizes used in this project. Toughened glass in frames was able to reach 40 kW/m^2 and above, especially when detail is payed to reducing the number of flammable components. See Trend test methodology in Appendix B1.

Figure 21 shows the results of framed experiments versus the radiation profiles used. As can be seen, 5 mm toughened glass was the best performer, with many tests reaching 40 kW/m^2 and those in aluminium frame fail on cool down or well after the tests are finished and are not represented here on this graph.

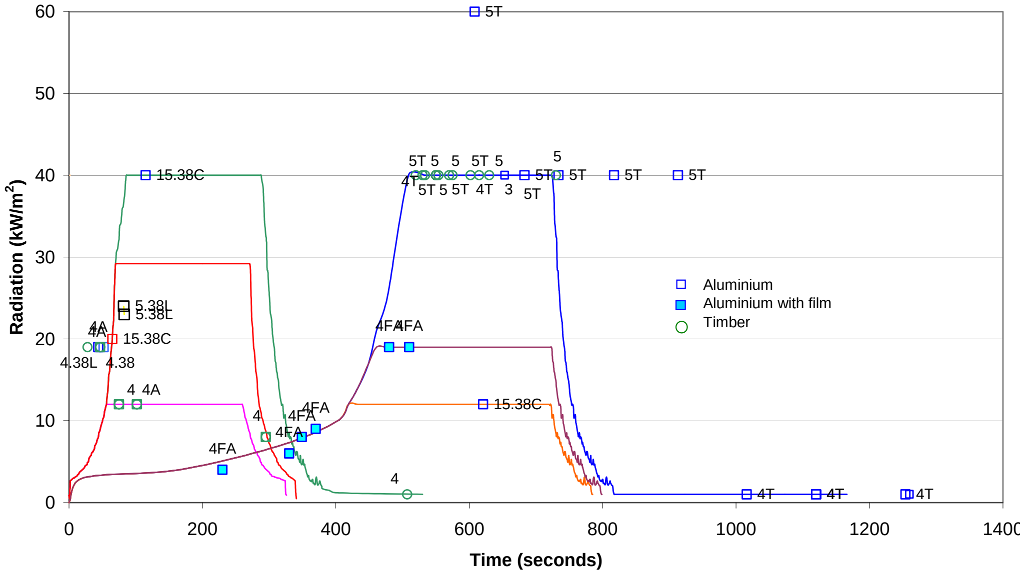

Figure 21. Radiation profiles versus framed glazing failure.

8.3.5 Film on glazing

Reflective film usage on glazing has beneficial effects generally related to its thermal effects in reducing heat loss or gain from a dwelling. Its performance under bushfire simulated exposure was investigated Bekaert P/L had proprietary Solagard films placed on 4 mm annealed glass in generic CRC aluminium frames (see Appendix B3 for further details). Low levels of radiation exposure showed little performance improvement on annealed glass without surface treatment.

The reduction of back face radiation is a plus for films, but annealed glass has a low exposure threshold and the addition of the films used generally showed insignificant gains in glazing performance. However, the performance of films when placed externally was significant. Lower thermal exposure of glazing by reflection of film on the front face increased thermal exposure before first crack from 9 to 27 kW/m^2. The use of metallic films is advised as they tend to hold their shape, thus supplying mechanical assistance to glass and reducing the chance of glass fall out.

In the Canterbury tests, one experiment with film on 4 mm annealed glass in their proprietary timber, Meranti, frame. These results showed insignificant change from the results expected from unfilmed glass due to the flaming of the window frame, (see Appendix B2 for further description).

9. Future Work

9.1 Framing effects

There appears to be many issues unexplainable at this time concerning timber frames.

A series of experiments is proposed in the near future on timber frames. Two factors are to be investigated. Firstly the effect frame rebate dimension shading and its equal shading by matching beading on glass failure. With this the issue of mechanical restraint of fixture and the heat sink effects of frame dimensions are to be explored.

Glass as a flexible material under thermal load must have constraint enough to keep it in place within the frame but must not be constrained enough that fixing alone contributes to its failure whilst it is thermally expanding.

This and the effect of glass shading, by rebate dimensions, is yet to be explored.

Further there is an effect in place by heat soak through the frame. Future experiments hope to show what effects if any are contributing factors on glazing failure when frame sizes are altered. This is to be achieved by changing frame width and thickness whilst maintaining same rebate dimensions.

9.2 Fire retardancy

There is much work being carried out by various organisations and manufacturers to develop fire retardants for new works and retrofitting. Aluminium tape usage on frames in this current experimentation has been used as a 'mock' retardant simulation showing an affect on the delay of ignition and failure times.

Experimentation has shown that frame flaming can lead to the early onset of glazing failure.

Testing of timber framing and its flammability, whether under retardant treated or not is currently defined under AS3959 is determined by cone calorimetry tests. A peak of 100 kW/m^2 is not to be exceeded nor an average of 60 kW/m^2 of Heat release during the 10 minutes after ignition of said timber.

Future works may show that a more systematic approach should be adopted whereby a window system is tested under bushfire loading rather than looking at individual componentry such as the timber frame. On current Standards flaming of a timber frame would fail a window system whether the glass failed or not.

Flaming of materials can occur without sufficient enough energy to ignite surrounding componentry so this should be considered. As an impractical analogy candles and paper can be ignited but they don't have enough heat energy to ignite a piece of framing timber and create sustained flaming.
Using bushfire profiling and different window systems may lead us to different assumptions on radiation, flammability and window system failure, their radiation levels and particularly failure times.

Retardant systems which include coatings resist radiation exposures but their service life is a factor which needs to be considered. In particular at what point are they needed to be replenished or retrograded and what are the tell tale signs a homeowner needs to look for to be aware. There is an important role to play here by manufacturers guaranteeing products and authorities ensuring all participants are aware of service life and retreatment times.

There are assumptions made as to the service life of retardants which are not easily proven or negated because a history is required to make informative judgement decisions on such matters.

9.3 Window screening

AS3959 prescribes an aperture size less than or equal to 1.5 mm aperture to stop embers. The fineness of mesh, colour, potential for thermal degradation, and guage of wire can be specified to provide usefulness in the case of ember attack however can dwelling occupants still get the view from their living room that they require? A compromise will take time but must be investigated.

10. Conclusions

10.1 Radiation exposure

In this investigation it was shown that the peak exposure of glazing and or glazing systems to radiation and related thermal effects have a marked effect on failure.

Initial radiation exposures where constrained by the test equipments ability. On modification bushfire radiation profiles developed in previous experimentation were able to be employed. These slow and fast bushfire exposures better reflect the reality of exposure to bushfire employing radiation as the defining factor in a time based profile. Testing normally carried out in window/glazing tests employs a time v. temperature curve as in AS1530.4. Time temperature v. curves are more commonly employed to relate to window failure where building to building or storey to storey flame spread of window failures occur due to compartment fires and don't relate directly to bushfire failure.

Bushfire failure of windows can lead to the entry of embers or the flammability of internal componentry but in isolated locations the chance of house to house spread can be a non issue. The key issue is considering each dwelling as a singular and reducing the chance of any failure that might compromise the building envelope.

If the information and recommendations of this report are adopted the question of which radiation profile reported here is to be adopted or should another be adopted.

The use of bushfire radiation profiles allows for deemed to comply methodology in testing which if well documented could be accepted by authorities in the future as an acceptable approach to window system specification in bushfire prone areas.

10.2 Glass fixture

10.3 Glass specification

This proves to be a difficult decision. The selection of glass type or thickness is greatly effected by its envelope. Testing in this investigation has shown that thickness plays an effect as does glass type.

The interesting effect in this investigation is glass performance when unframed. Results of tests were quite spread as to when crack or shatter occured.

It was noticed visually but not measured in this investigation that glass flexes during radiation exposure. This was most noticeable in unframed tests, measurements of flexure not taken. Existing Standards on glazing specification take into account mechanical loading on glazing especially by wind. Flexure by bushfire exposure however may add a different component to the equation.

Timber framing methodology employs the use of silicone sealant which acts as a weatherproofing medium and as some glaziers will tell holds the window in place before the timber beading is nailed or stapled into place. However under wind loading this creates a mechanical elastic joint for window edging. In a bushfire exposure it is possible that the mechanical strength of this can be compromised on heating. If glass flexure can increase it may increase the performance of glass under exposure to bushfire but should flammability of silicone and surrounding components occur it may have a detrimental effect by supplying large variation on edges by thermal loading due to flaming and shading.

The investigation of glazing performance in this project was to look at key points affecting the performance of glazing systems under the exposure regimes that a bushfire would place on a window. The rate of exposure, wait times in radiation profiles and piloting are all major factors effecting performance. Flaming of window rubber may not occur if piloting is not present. The likelihood of failure of windows on the flaming of componentry is increased. Trend window testing showed that systematic replacement of flammable components increases the survivability of windows under bushfire exposures.

The outcomes of this work are in no way a definitive answer on window design in bushfire-prone areas, but has attempted to highlight points of consideration for those designing windows in the future.

Glass selection and frame type are of course key components. However, the Trend series of tests showed that changing detail and removing flammable componentry can greatly effect the performance of a window.

Keski–Rahkonen [9] identified that temperature differences between the heated glass surface and the edge-shielded glass in a window played a large role in controlling glass cracking. It is hoped future works will further clarify this.

The variation of work done by others referenced is not readily applicable to the approach of bushfire research. The approach taken in this experimentation yielded different results to other test methods, but best represents a ‘real’ bushfire.

11. References

1. Australian Standard AS 3959–1999, *Construction of Buildings in Bushfire-Prone Areas*, Standards Australia, Sydney.
2. Harada, K., Enomoto, A., Uede, K. & Wakamatsu, T. 2000, An experimental study on glass cracking and fallout by radiant heat exposure, in *Fire Safety Science – Proc. 6th Int. Symp.*, pp. 1063–1074, International Association for Fire Safety Science, London, UK.
3. Mowrer, F.W. 1998, *Window Breakage Induced by Exterior Fires*, NIST-GCR-98-751, National Institute of Standards and Technology, Gaithersburg, MD, USA.
4. Cohen, J.D. & Wilson, P. 1994, Current results from structure ignition assessment model (SIAM) research, presented to Fire Management in the Wildland/Urban Interface: Sharing Solutions Conf., Kananaskis, Alberta, Canada, 2–5 October.
5. McArthur, N.A. 1991, The performance of aluminium building products in bushfires, *Fire & Materials*, **15**, 117–125.
6. Shields, T.J., Silcock, G.W.H. & Flood, M.F. 2001, Performance of a single glazing assembly exposed to enclosure corner fires of increasing severity, *Fire & Materials*, **25**, 123–152.
7. Pagni, P.J. & Joshi, A.A. 1991, Glass breaking in fires, in *Fire Safety Science – Proc. 3rd Int. Symp.*, p. 791, International Association for Fire Safety Science, London, UK.
8. Australian Standard AS 1530.4–1997, Methods for Fire Tests on Building Materials, Components and Structures: Part 4 – Fire Resistance Tests of Elements of Building Construction, Standards Australia, Sydney.
9. Keski–Rahkonen, O. 1988, Breaking of window glass close to fire. *Fire & Material*, **12**, 61–69.
10. Babrauskas, V. 2005, *Glass Breakages in Fires*, Fire Science & Technology Inc., Issaquah, WA, USA [http://www.doctorfire.com/glass.html; accessed July 2005).
11. Hassani, S.K.S., Shields T.J. & Silcock, G.W. 1994–95, Thermal fracture of window glazing: performance of glazing in fire. *J. Applied Science*, **4**(4), 249–263.
12. Australian Standard AS 1288–1994, *Glass in Buildings – Selection and Installation*, Standards Australia, Sydney.
13. Australian Standard AS 2047–1999, *Windows in Buildings – Selection and Installation*, Standards Australia, Sydney.
14. Australian Standard AS 4055–1992, *Wind Loads for Housing*, Standards Australia, Sydney.
15. Sincaglia, P.E. & Barnett, J.R. 1997, *J. Fire Protection Engg*, **8**(3), 101–118.

Appendix A – All Test Results

Tables Legend

Failure modes:	a: Breach of integrity b: Glass cracking
Glazing notes:	R = failed on return, C = failed on cooling An/toughened = 3 mm plain external and 6.38 mm laminated Frontline glass with a 6mm air gap between
Frame type:	A: Aluminium frame – CRC B: Timber frame (CRC A), oregon and Tasmanian oak beading C: Timber frame (CRC B), KDHW frame and Tasmanian oak beading D Timber frame (CRC B), all timber surfaces were coated in aluminium tape E: Trend – aluminium Quantum awning sash/sliding channel, glazed F: Trend – aluminium sash/sliding channel, glazed G: Trend – aluminium Quantum awning sash/sliding channel, glazed (2 lights wide) H: Trend – aluminium sash/sliding channel, glazed (2 lights wide) I: Canterbury – timber frame 1057 × 915 meranti awning window J: 20 mm aluminium tape around edge
Profiles:	A: 30 Hz speed = 0.03 m/s with 10 s wait at panel B: 30 Hz speed = 0.03 m/s with 30 s wait from cold start specimen C: Shock tests at 12.5 kW/m^2 D: Shock test at 19 kW/m^2 E: Fast profile following bushfire curve F: Slow profile following bushfire curve G: 10 Hz speed = 0.01 m/s H: 60 Hz speed = 0.07 m/s
Glass treatment:	A: Glass sponged with a weak hydrated lime solution (10%) B: Arc mesh 6037 stainless steel flyscreen C: Bekaert film – ST70A D: Bekaert film – EXTS20 E: Bekaert film (type unknown) F: Bekaert film – Clear G: Bekaert film – Silver 20 H: Bekaert film – Sterling 60

Table A1. Unframed glazing test results

Specimen no.	Glass	Thick-ness (mm)	Glass treat-ment	Frame type	Window seal	Sash (fixed/ open)	Test profile	Radiation (kW/m^2)				Temperature (°C)		Time to flaming (s)	Failure mode	Glass failure 1st crack (s)
								Peak at failure	Peak Rad 1	Peak Rad 2	Peak back face	Peak front face	Peak back face			
4PL30A	Annealed	4	No	No	No	No	A	60	60	67	13	641	190	No	Crack	114
4PL30B	Annealed	4	No	No	No	No	A	60	20	22	9	284	255	No	Crack	138
4PL30C	Annealed	4	No	No	No	No	A	40	24	26	11	232	245	No	Crack	139
4PL30D	Annealed	4	No	No	No	No	A	40	41	43	15	255	275	No	Crack	155
4PL30E	Annealed	4	A	No	No	No	A	12R	9	12	6	211	260	No	Crack	159
AN3A30W30	Annealed	4	No	No	No	No	B	50	50	50	12	257	167	No	Crack	117
AN45A10	Annealed	4	No	No	No	No	G	124	22	24	9	171	180	No	Crack	317
AN45A60	Annealed	4	No	No	No	No	B	No	40	36	10	160	116	No	No	No
AN45B10	Annealed	4	Corrupt data file	No	No	No	G	No						No	No	No
AN45B60	Annealed	4	No	No	No	No	H	No	44	40	12	163	148	No	No	No
AN45C(10HZ)	Annealed	4	No	No	No	No	G	No	22	22	23	96	91	No	No	No
AN45C60	Annealed	4	No	No	No	No	H	No	44	39	13	122	86	No	No	No
AN45D10	Annealed	4	No	No	No	No	G	24	26	24	8	172	162	No	Crack	313
AN45E(10HZ)	Annealed	4	No	Data ended at 293 s	No	No	G	1C						No	Crack	1382 shatter
AN5A30TF6037	Annealed	4	Mesh		No	No	G	1C	12	12	9	69	53	No		158R
5LA30A	Laminated	4.38	No	No	No	No	B	73	69	73	7	422	186	No	Crack	130
L10A30W30	Laminated	10	No	No	No	No	B	38	53	38	6	249	83	No	Crack	122
L5A10	Laminated	5.38	No	No	No	No	G	12	18	12	5	98	94	No	Crack	224
L5A30	Laminated	5.38	No	No	No	No	B	19	35	22	6	105	73	No	Crack	84
L5A30E20	Laminated	5.38	No	20 mm foil	No	No	B	17	25	17	5	81	60	No	Crack	78
T4A10E20	Toughened	4	No	No	No	No	G	No	41	28	15	119	91	No	No	No
T4A30E20	Toughened	4	No	No	No	No	H	No	42	29	16	129	98	No	No	No
5T30A	Toughened	5	No	No	No	No	B	68	66	68	10	314	169	No	Crack	130

Table A2. Timber framed results

Specimen no.	Glass	Thick-ness (mm)	Glass treat-ment	Frame type	Window seal	Sash (fixed/ open)	Test profile	Radiation (kW/m²) Peak at failure	Peak Rad 1	Peak Rad 2	Peak back face	Temperature (°C) Peak front face	Peak back face	Time to flaming (s)	Failure mode	Glass failure 1st crack (s)
4LATSH12	Annealed	4	No	Timber B	No	No	C	12	10	12	3	102	104	No	Crack	75
4PLTSH12	Annealed	4	No	Timber B	No	No	C	12	10	12	5	100	120	No	Crack	102
4PLTSH19	Annealed	4	No	Timber B	No	No	D	19	15	19	7	100	94	No	Crack	47
4LTSH19	Laminated	4.38	No	Timber B	No	No	D	20	16	20	3	76	92	No	Crack	28
L5B30TF3032	Laminated	5.38	No	Timber A	No	No	B	20	19	20	6	102	70	No	Crack	94
L5A30TF6037	Laminated	5.38	No	Timber A	No	No	B	14	12	14	3	99	65	No	Crack	105
L5A30AL	Laminated	5.38	No	Alum A	No	No	B	16	35	16	7	137	100	No	Crack	83
L5A30TF	Laminated	5.38	No	Timber A	No	No	B	23	23	23	5	92	59	No	Crack	82
L5A30TF1628	Laminated	5.38	No	Timber A	No	No	B	23	13	23	4	29	64	No	Crack	97
L5A30TF3032	Laminated	5.38	No	Timber A	No	No	B	16	15	16	5	124	5	No	Crack	105
4TTFA40	Toughened	4	No	Timber C	No	No	F	40	24	15	10	233	194	538	Crack	507
4TTFB40S	Toughened	4	No	Timber C	No	No	F	40	45	26	20	428	319	583	Smash	765
4TTFC40S	Toughened	4	No	Timber C	No	No	F	40	47	25	17	416	299	498	Smash	530
4TTFD40S	Toughened	4	No	Timber C	Black silicone	Fixed	F	40	37	26	50	477	287	480	Smash	520
4TTFS40S	Toughened	4	No	Timber C	Foil in rebate	Fixed	F	?C	46	26	20	542	302	566	Smash	?C
Canter 1	Toughened	5	No	Timber I	No	Open	F	40	60	42	50	383	291	515	Crack	554
Canter 2	Toughened	5	No	Timber I	No	Open	F	40	60	35	15	369	280	518	Crack	534
Canter 3	Toughened	5	E	Timber I	No	Open	F	19	8	8	3	141	128	No	Crack	295
6TFA40F	Toughened	6	No	Timber C	No	fixed	E	No	49	38	11	296	225	No	No	No
5TSH40	Toughened	5	No	Timber B	No	fixed	H	No	48	46	11	237	145	No	No	No
5TTF29AC	Toughened	5	No	Timber C	No	No	F	No	31	25	14	361	333	No	No	No
5TT40C	Toughened	5	No	Timber D	No	No	F	40	57	44	17	401	339	No	Smash	630
5TT40A	Toughened	5	No	Timber C	No	No	F	40	60	42	16	385	303	520	Smash	570
5TT40B	Toughened	5	No	Timber C	Silicone	No	F	40	67	42	15	380	293	523	Smash	550
5TT40D	Toughened	5	No	Timber C	No	No	F	40	67	39	16	388	299	495	Smash	550
6TTFB40S	Toughened	6	No	Timber D	No	No	F	40	46	27	17	407	319	No	Crack	615
Film 7	Annealed	4	F	Timber C	Rubber	No	F	No	15	11	9	286	282	No	No	No
5TTFR40A	Toughened	5	No	Timber C	No	No	F	No	67	41	21	429	385	490	No	No
5TTALR40	Toughened	5	No	Timber C	No	No	S	20	38	20	13	336	254	687	Smash	730
5TTALR40B	Toughened	5	No	Timber C	No	No	S	40	73	30	15	560	268	730	No	No
5TTALR40C	Toughened	5	No	Timber C	No	No	S	40	46	34	18	486	337	507	No	No
5TTALR40D	Toughened	5	No	Timber C	No	No	S	40	46	34	16	501	296	502	Smash	575
5TTALR40E	Toughened	5	No	Timber C	No	No	S	40	63	33	14	426	253	477	No	No
5TTALRF	Toughened	5	No	Timber C	No	No	S	40	59	33	14	506	287	490	Smash	550

Table A3. Aluminium framed results

Specimen no.	Glass	Thick-ness (mm)	Glass treat-ment	Frame type	Window seal	Sash (fixed/ open)	Test profile	Radiation (kW/m^2) Peak at failure	Peak Rad 1	Peak Rad 2	Peak back face	Temperature (°C) Peak front face	Peak back face	Time to flaming (s)	Failure mode	Glass failure 1st crack (s)
Film 1	Annealed	4	F	Alum F	Rubber	No	F	4	6	4	1	109	102	No	Crack	230
Film 2	Annealed	4	G	Alum F	Rubber	No	F	5	7	5	1	134	146	No	Crack	330
Film 3	Annealed	4	H	Alum F	Rubber	No	F	No	17	10	8	281	273	No	No	No
Film 4	Annealed	4	F	Alum F	Rubber	No	F	No	16	11	8	266	269	No	No	No
Film 5	Annealed	4	F	Alum F	Rubber	No	F	No	15	10	8	277	276	No	No	No
Film 6	Annealed	4	F	Alum F	Rubber	No	F	No	14	11	9	281	207	No	No	No
Film 8	Annealed	4	G	Alum F	Rubber	No	F	No	15	11	3	254	203	No	No	No
Film 9	Annealed	4	G	Alum F	Rubber	No	F	No	25	17	5	327	265	No	No	No
Film 10	Annealed	4	C	Alum F	Rubber	No	F	20	9	6	2	143	139	No	Crack	370
Film 11	Annealed	4	C	Alum F	Rubber	No	F	20	8	5	2	146	127	No	Crack	349
Film 12	Annealed	4	D	Alum F	Rubber	No	F	20	23	15	3	217	162	No	Crack	510
Film 13	Annealed	4	D	Alum F	Rubber	No	F	27	27	15	2	211	157	No	Crack	480
4PLALSH12	Annealed	4	No	Alum A	No	No	C	No	10	13	4	121	108	???	No	No
4PLALSH19	Annealed	4	No	Alum A	No	No	D	19	17	22	7	46	50	???	Crack	44
3TALSA	Toughened	3	No	Alum A	Rubber	Fixed	F	No	27	22	12	250	238	No	No	No
3TALSB	Toughened	3	No	Alum A	Rubber	Fixed	F	No	37	22	21	382	333	No	No	No
3TFC40S	Toughened	3	No	Alum A	Rubber	Fixed	F	1C	46	27	21	402	133	No	Fell in frame	1260C
3TFA40S	Toughened	3	No	Alum A	Rubber	No	F	40	50	40	18	393	356	No	Smash	653
3TFB40S	Toughened	3	No	Alum A	Rubber	No	F	No	39	23	24	428	378	No	No	No
3TFC40S	Toughened	3	No	Alum A	Rubber	No	F	1C	45	26	21	395	113	604	Smash	1260C
4TFB40	Toughened	4	No	Alum A	No	No	F	No	43	34	10	218	159	No	No	No
3TALB40	Toughened	4	No	Alum A	Rubber	Fixed	F	1C	46	26	27	448	433	550	Smash	1016R
4TFA12	Toughened	4	No	Alum A	Rubber	No	B	No	16	13	4	147	132	No	No	No
4TFA40	Toughened	4	No	Alum A	Rubber	No	B	No	65	50	21	359	318	???	No	No
4TFB40S	Toughened	4	No	Alum A	Rubber	No	F	No	55	43	19	395	354	???	No	No
4TALA40	Toughened	4	No	Alum A	Silicone	No	F	No	47	27	24	469	388	550	No	No
4TALB40	Toughened	4	No	Alum A	Silicone	No	F	No	42	26	22	458	432	555	No	No
4TALC40	Toughened	4	No	Alum A	Silicone	No	F	No	75	24	19	367	328	560	No	No
Trend 3	Toughened	4	No	Alum F	Rubber	Open	E	No	41	45	23	394	402	No	No	No
Trend 5	Toughened	4	No	Alum E	Rubber	Open	F	40	39	45	19	330	306	?	Crack	690
Trend 6	Toughened	4	No	Alum F	Rubber	Open	F	1C	40	49	24	421	419	810	No	5 min post-test
5TAL40	Toughened	5	No	Alum A	Silicone	No	F	No	59	42	23	450	428	No	No	No
5TALA40	Toughened	5	No	Alum F	Rubber	No	F	1C	41	24	15	323	277	560	Smash	1130C
5TALSH19	Toughened	5	No	Alum A	No	No	D	No	23	23	6	110	91	No	No	No
5TFA40F	Toughened	5	No	Alum A	Rubber	No	E	No	51	40	15	364	310	No	No	No

Specimen no.	Glass	Thick-ness (mm)	Glass treat-ment	Frame type	Window seal	Sash (fixed/ open)	Test profile	Radiation (kW/m^2)				Temperature (°C)		Time to flaming (s)	Failure mode	Glass failure 1st crack (s)
								Peak at failure	Peak Rad 1	Peak Rad 2	Peak back face	Peak front face	Peak back face			
5TFA40S	Toughened	5	No	Alum A	Rubber	No	F	1C	63	47	23	442	412	No	No	800R
Trend 1	Toughened	5	No	Alum E	Rubber	Open	E	No	37	43	16	339	309	No	No	No
Trend 2	Toughened	5	No	Alum F	Rubber	Open	E	No	38	40	10	191	147	No	No	No
Trend 8	Toughened	5	No	Alum E	Rubber	Open	E	1C	43	44	20	422	246	156	No	2.5 hour post-test
Trend 9	Toughened	5	No	Alum H	Rubber	Open	E	1C	40	39	12	365	240	230	No	4 min post-test
Trend 10	Toughened	5	No	Alum G	Rubber	Open	E	No	41	40	11	365	265	165	No	No
Trend 12	Toughened	5	No	Alum E	Silicone	Open	F	40	45	25	22	403	264	734	742 s internal flaming	No
Trend 13	Toughened	5	No	Alum E	Silicone	Open	E	40	39	24	17	328	317	240	No	No
Trend 14	Toughened	5	No	Alum E	Silicone	Open	E	No	39	24	19	193	272	No	No	No
Trend 15	Toughened	5	No	Alum E	Silicone	Open	F	No	41	24	22	351	409	No	No	No
Trend 16	Toughened	5	No	Alum F	Silicone	Open	F	No	38	24	17	351	318	735	No	No
Trend 17	Toughened	5	No	Alum E	Silicone	Open	F	No	46	26	18	473	428	692	817 s internal flaming	No
Trend 18	Toughened	5	No	Alum E	Silicone	Open	F	No	46	25	19	438	361	625	No	No
Trend 19	Toughened	5	No	Alum E	Silicone	Open	F	No	46	27	19	415	313	No	No	No
Trend 20	Toughened	5	No	Alum F	Silicone	Open	F	40	46	25	20	430	386	904	913 s internal flaming	No
Trend 21	Toughened	5	No	Alum F	Silicone	Open	F	40	46	24	19	420	380	683	683 s internal flaming	No
Trend 22	Toughened	5	No	Alum F	Silicone	Open	F	No	50	24	21	443	398	No	No	No
Trend 23	Toughened	5	No	Alum F	Silicone	Open	F	No	44	23	19	390	373	No	No	No
Trend 24	Toughened	5	B	Alum F	Silicone	Open	E	No	67	40	18	509	370	314	No	No
Trend 25	Toughened	5	No	Alum F	Silicone	Open	F	60	64	38	42	368	272	No	Shatter	576 shatter
6TFA40F	Toughened	6	No	Alum A	Rubber	No	E	No	51	40	16	394	340	No	No	No
Trend 11	An/toughened	15.38	No	Alum G	Rubber	Open	E	22	22	20	1	95	32	150	Crack	65
Trend 7	An/toughened	15.38	No	Alum G	Rubber	Open	F	11	9	11	1	163	74		Crack	621
Trend 4	An/toughened	15.38	No	Alum G	Rubber	Open	E	40	38	39	1	253	51	No	Crack	115
L5B30ALW30	Laminated	5.38	No	Alum A	No	No	B	19	23	16	6	81	59	No	Crack	82

Appendix B – Proprietary Glazing Tests

B1. Trend Windows

B1.1 General

Trend Windows supplied some of their proprietary windows for testing in our bushfire simulations. The aim of the exercise was to supply them with information that would better enhance their existing framing systems, Trend and Quantum. Windows supplied were either awning or sliding single units, or sliding and fixed pane combinations. All windows tested had aluminium components.

Single glazed units were typically 1035 × 840 mm overall. Double glazed units were 1035 × 1520 mm.

Trend 1–7 specimens were single glazed units with no timber reveal; all units supplied after these were supplied with timber (meranti) reveals.

The majority of the windows tested contained 5 mm toughened glass, the exceptions being Trend 4, 7 and 11, which contained a combination glazing system. This combination glazing system was 15.38 mm thick and consisted of 3 mm annealed glass, a 6 mm air gap and 6.38 mm laminated Frontrunner glass. The annealed glass is always on the outside of the window and thus is on the test face.

B1.2 Results and discussion

B1.2.1 Series 1 Tests: Trend 1–11

The data from these tests is reported in Table B1. Trend 1–3 had no flaming or failure of these single light units. Trend 4 was the first glazing failure, as expected, with the 3 mm annealed glazing failing at 37 kW/m^2. It is important to note that the fast bushfire profile was applied to these tests which does not allow for the worst-case slow profile to build heat within all window members, which could have brought about the onset of flaming or even earlier glazing breakage. The effect of slow profile versus fast is highlighted in Trend 4 and 7, which had the same componentry. However, the 3 mm annealed glass broke at 8 kW/m^2 under the slow profile, compared to 37 kW/m^2 under the fast profile. The slow profile is the more punishing and offers the best exposure for a worst-case scenario fire build up.

Trend 5 was the first of the failures involving glazing installation methods. The 4 mm glazing was in no way affected by the radiation load imposed, as there was no physical observation of cracking etc. Rubber seals/beads which held the glazing into the aluminium profiles melted under the heat/radiation loading. The rubber, especially at the top, melted and ran down the window face. This rubber then ignited at 690 s whilst under a radiation loading of 38kW/m^2. The failure of the rubber would not have been of concern if it had been confined to the outside of the window, however it also ignited on the internal window face. Flame spread internally in this experimentation is considered a fail as there is the chance of ignition from this flaming of internal dwelling fixtures, such as curtains. Figure B1 shows this flaming for Trend 6.

Table B1 – Results of Trend window tests

Specimen no.	Glass	Thick-ness (mm)	Glass treat-ment	Window seal	Test profile	Failure radiation (kW/m^2)	Test peak radiation, Rad 1 top (kW/m^2)	Test peak radiation, Rad 2 bottom (kW/m^2)	Peak back face radiation (kW/m^2)	Peak front face temp. (°C)	Peak back face temp. (°C)	Time to flaming (s)	Failure mode	Glass failure 1st crack (s)
Trend 1	Toughened	5	No	Rubber	E	No	37	43	16	339	309	No	No	No
Trend 2	Toughened	5	No	Rubber	E	No	38	40	10	191	147	No	No	No
Trend 3	Toughened	4	No	Rubber	E	No	41	45	23	394	402	No	No	No
Trend 5	Toughened	4	No	Rubber	F	40	39	45	19	330	306	?	Crack	690
Trend 6	Toughened	4	No	Rubber	F	1C	40	49	24	421	419	810	No	5 min post-test
Trend 8	Toughened	5	No	Rubber	E	1C	43	44	20	422	246	156	No	2.5 hour post-test
Trend 9	Toughened	5	No	Rubber	E	1C	40	39	12	365	240	230	No	4 min post-test
Trend 10	Toughened	5	No	Rubber	E	No	41	40	11	365	265	165	No	No
Trend 12	Toughened	5	No	Silicone	F	40	45	25	22	403	264	734	742 s internal flaming	No
Trend 13	Toughened	5	No	Silicone	E	No	39	24	17	328	317	240	No	No
Trend 14	Toughened	5	No	Silicone	E	No	39	24	19	193	272	No	No	No
Trend 15	Toughened	5	No	Silicone	F	No	41	24	22	351	409	No	No	No
Trend 16	Toughened	5	No	Silicone	F	No	38	24	17	351	318	735	No	No
Trend 17	Toughened	5	No	Silicone	F	40	46	26	18	473	428	692	817 s internal flaming	No
Trend 18	Toughened	5	No	Silicone	F	No	46	25	19	438	361	625	No	No
Trend 19	Toughened	5	No	Silicone	F	No	46	27	19	415	313	No	No	No
Trend 20	Toughened	5	No	Silicone	F	40	46	25	20	430	386	904	913 s internal flaming	No
Trend 21	Toughened	5	No	Silicone	F	40	46	24	19	420	380	683	683 s internal flaming	No
Trend 22	Toughened	5	No	Silicone	F	No	50	24	21	443	398	No	No	No
Trend 23	Toughened	5	No	Silicone	F	No	44	23	19	390	373	No	No	No
Trend 24	Toughened	5	B	Silicone	E	No	67	40	18	509	370	314	No	No
Trend 25	Toughened	5	No	Silicone	F	40	64	38	42	368	272	No	Shatter	576 shatter
Trend 11	Pl/toughened	15.38	No	Rubber	E	20	22	20	1	95	32	150	Crack	65
Trend 4	Pl/toughened	15.38	No	Rubber	E	40	38	39	1	253	51	No	Crack	115
Trend 7	Pl/toughened	15.38	No	Rubber	F	12	9	11	1	163	74		Crack	621

Figure B1. Flaming of rubber beading – Trend 6.

Trend 6 failed in much the same way as Trend 5, but showed a second failure mode. This second failure mode occurred in some other tests using toughened glass. The glazing did not fail during the test cycle, but shattered on cooling. In this case, it was 300 s after the test was completed and was a surprise to all. This type of failure highlights a safety issue that can occur after the firefront has passed. This raises the question that if this failure mode is acceptable, then what duration after the firefront passes is this deemed acceptable?

Trend 8 and all subsequent tests were piloted with a flaming timber stick. This was to better simulate the potential ignition of volatiles off-gasing during the heating phase when these volatiles have flame impingement. This test was a repeat of Trend 1, but with the timber reveal and the piloted ignition.

The addition of the piloting, which simulates a more realistic scenario, led to the ignition of the volatiles from the rubber beading at 156 s. This then spread the flaming to the seals between the window and its frame. Flaming of internal seals led to flame impingement of the window’s back face, thus increasing the mechanism of rubber bead flaming internally. The window shattered 2.5 hours after the end of the test.

Trend 9 and 10 had the same failures (see Figures B2 and B3), whereby flaming of rubber and foam seals led to internal flame spread. Trend 11 had the same framing system as Trend 10, but was glazed using the 15.38 mm glazing combination.

The failure mode of Trend 11 was the same as Trend 4 and 7. The weak link in Trend 11 was the 3 mm annealed glass, which cracked at 23 kW/m^2. The specimen did not ignite until much later, but when it did the failure mode was the same.

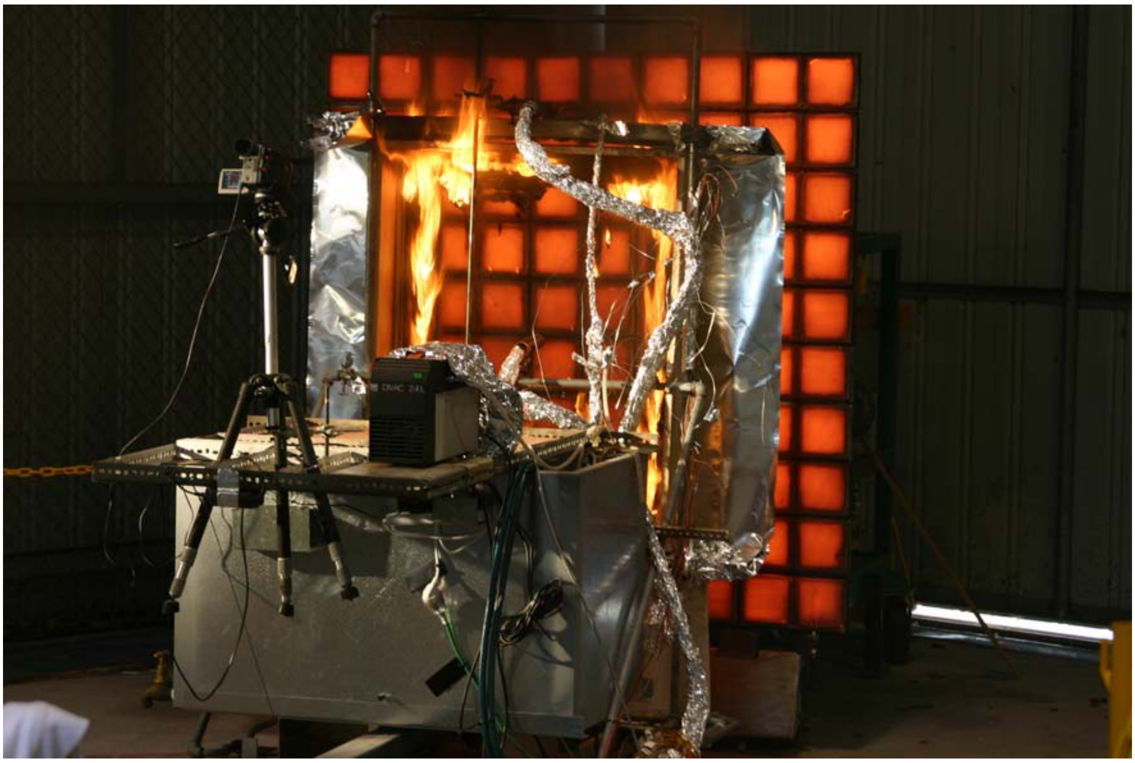

Figure B2. Flaming of seals – Trend 8.

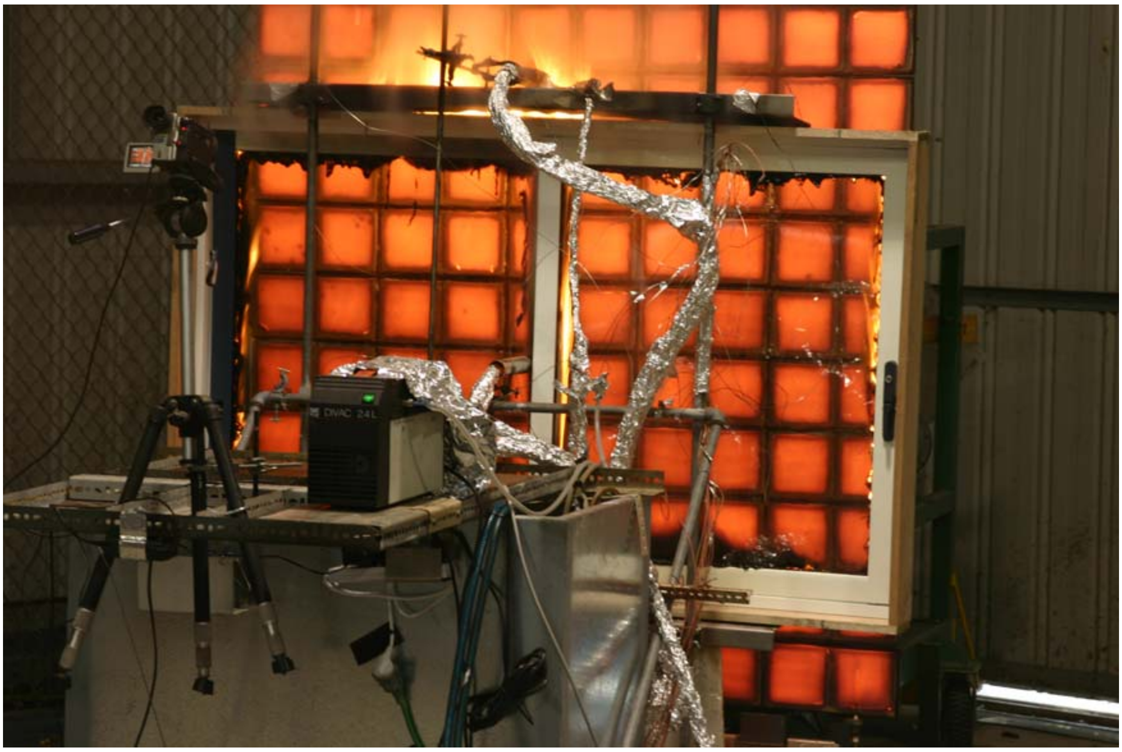

Figure B3. Flaming of double light unit – Trend 10.

B1.2.2 Series 2 Tests: Trend 12–16

From the previous series of tests, it was noted that one of the main contributors to the flaming of windows was melting rubber seals and their ultimate ignition, thus adding to the stress imposed on a system by providing further heat exposure.

As a result of this, new glazing seals were made from silicone rubber to replace the standard rubber beading used. The silicone rubber has been successfully used as a replacement in previous research work, having a higher fire performance rating.

Trend 12–16 were Quantum windows. Trend 12 was a single glazed window that ignited at 716 s at a measured radiation of 46 kW/m^2. The silicone beading did not flame however the central rubber weatherstop between the interlockers off-gased. Eventually, flaming of this occurred and progressed over the top and also burnt up through the seal, causing flaming on the inside of the window unit.

In Trend 13 the foam weatherstop flamed, as did the rubber bungs which were in the ends of the vertical window members. Flaming of the bungs created a fire in the window section, creating a chimney effect that allowed flames to breach the upper window, thus allowing flaming to spread to the internal side of the window. The bungs were removed for progression of testing to Trend 14. For Trend 14, the foam weatherstop was replaced with 5 mm diameter silicone tubing to create a non-flaming weatherseal. As a result, there was no flaming in this test and no window failure, as was the case for Trend 15.

Trend 16 was a double light unit that was placed centrally on the test rig. This specimen flamed, and the source of this flaming was the interlocker seal which melted, forming a fire that breached the sections, allowing internal flaming.

B1.2.3 Series 3 Tests: Trend 17–25

Trend 17, an awning window, flamed at 817 s, allowing flames to spread internally. It was later discovered that the window seals flamed and that flame spread was enhanced because the window was not completely shut.

Trend 18 flamed, but not from any of the seals but from the powder coating, a mid-blue colour, on the central mullion.

Trend 19 was a repeat of the window used in Trend 12. The removal of all potential flaming seals resulted in a test to 45 kW/m^2 with no flaming and no glass failure.

Trend 20 and 21 had the same failure mode whereby the rubber bungs in the end sections flamed, allowing flames to spread to the back face of the window. In Trend 20, the gaps between the aluminium frame and the timber reveal were covered with aluminium tape to stop flame spread through this gap. The rubber bungs then became the weak link in this test.

Trend 22 was a repeat of the Trend 16 window. The central mullion was taped to the reveal, as was the opening where the interlocker seal was to stop any flaming. A peak radiation of 50 kW/m^2 was measured and no flaming occurred.

This approach was also carried out for Trend 23, a double light sliding window, and no flaming resulted.

Trend 24 reused the window from the Trend 23 test, but with a screen of 6037 stainless steel mesh placed over the front of the glazing unit. This mesh provides an open area of 35%. The mesh was spaced 10 mm from the outermost glass surface. Flaming did occur, but the attenuation of radiation of the mesh allowed this glazing unit to reach a measured exposure of 40 kW/m^2 at its centre and 67 kW/m^2 at the top of the glass of combined radiation and convective radiation, before the onset of flaming

Trend 25 was a repeat of the previous test using the same window. With all potential flaming componentry removed, this window reached 64 kW/m^2 at its top and approximately 40 kW/m^2 at its centre. Due to the feedback effects between the panel and specimens at radiation levels higher than 40 kW/m^2 due to their proximity, it is difficult to determine an exact radiation exposure level.

B1.3 Summary

The methodology used for this test series was to progressively work through the failure modes as they occur and replace componentry in order to stop initiation of failing. The testing carried out showed that it was possible to select an appropriate glass type, but this was only one factor to be considered.

Flaming componentry enabled breaches in window framing systems that allowed internal flaming to occur, which had the potential for flame spread to internal fixtures such as curtains.

The selection of 5 mm toughened glass was adequate for the tests for radiation loads to 40 kW/m^2. Trend 6, 8 and 9 didn’t fail during the tests, but broke post-test on cooling. Trend 8 surprisingly broke at 2.5 hours post-test.

Comparisons between Trend 24 and 25 show the effectiveness of window shading by flyscreens. Trend 24 had a back face radiation through the glass of 18 kW/m^2, which was less than half that of Trend 25. Also, the screening protected componentry in that, although flaming occurred, it did not assist any failure mechanism.

B2. Canterbury Windows

B2.1 General

The three windows tested were standard Canterbury awning windows, 1057 mm high by 915 mm wide with meranti frames. Frame moisture content was measured with a resistance moisture meter and was found to be between 9 and 10%.

B2.2 Results and discussion

Canter 1 and 2 were tested at radiation exposures of approximately 40 kW/m^2. From the data in Table B2, it can be seen that the radiation at cracking was 47 and 40 kW/m^2, respectively. These results reflect the performance that would be expected for 5 and 4 mm toughened glass. This data falls within the spread of data recorded for other timber frame tests. The onset of flaming of the timber frames increased the radiation to these levels, resulting in failure.

Table B2. Canterbury test results

Specimen no.	Glass	Thickness (mm)	Glass treatment	Window seal	Test profile	Failure radiation (kW/m^2)	Test peak radiation, Rad 1, top (kW/m^2)	Test peak radiation, Rad 2, bottom (kW/m^2)	Peak back face radiation (kW/m^2)	Peak front face temp. (°C)	Peak back face temp. (°C)	Time to flaming (s)	Failure mode	Glass failure, 1st crack (s)
Canter 1	Toughened	5	No	No	F	554	60	42	50	383	291	515	Crack	554
Canter 2	Toughened	5	No	No	F	534	60	35	15	369	280	518	Crack	534
Canter 3	Toughened	5	E	No	F	295	8	8	3	141	128	No	Crack	295

Canter 3, which was a 4 mm annealed glazing system with a 100 micron Bekaert film, cracked at 8 kW/m^2, which was significantly lower than measurements taken for the lowest unframed glazing, i.e. 22 kW/m^2 (4PL30B). However, similar performance for 4 mm annealed glass with film can be seen for aluminium frames (see Bekaert test results).

The Canter 3 test was continued after glass cracking to observe the spread of cracking and potential fall out of glazing. Glazing stayed intact and cracking continued around the edges of the glass, in particular in the region between where the film had shrunk or fallen away and the edge of the frame.

Figure B4 shows the radiation levels measured below the glazing in the non-flame zone. The rapid increase of temperature from flaming in the Canter 1 and 2 tests can be seen.

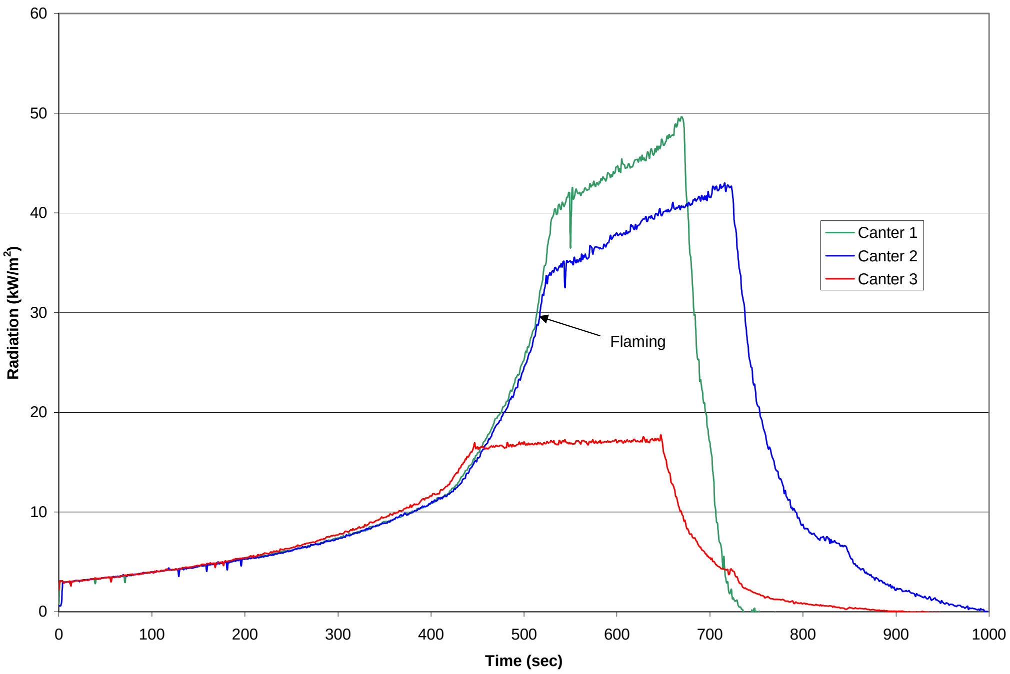

Figure B4. Radiation measured in Canter tests (Radiometer 2 – low).

It is important to note that the radiation measured was total radiation as measured by the total flux meters, and radiative and convective components cannot be separated. The rapid increase in the heat flux measured highlights the input from convective radiation.

The advantage of using a film on glazing, especially reflective, does have the bonus of reducing radiation passing through to the interior of buildings, thus reducing the chance of combustion of curtains and other furnishings. Interior films reflect some radiation received, creating extra re-radiation within the glass. This will effect glazing failure, but this aspect was not part of this investigation.

B2.3 Conclusions

The flaming of the frame is an issue that obviously adds to the thermal load on a window. If, in the case of these timber frames, flaming could be reduced then the maximum exposure could be increased. Fire-retardant coating on frames or higher density frames could delay or stop ignition, which may increase peak radiation loading, but this would need to be investigated further.

The one-off use of films and annealed glass in this investigation gives no conclusive results of glass and film interaction.

B3. Bekaert Films

B3.1 General

Various films (see Table B3) were tested to expected radiation levels of 19 or 29 kW/m^2. Films were placed over 4 mm annealed glass. There was no flaming of any of the componentry during these tests.

Table B3. Film testing results

Specimen no.	Glass	Thickness (mm)	Glass treatment	Window seal	Test profile	Failure fadiation (kW/m^2)	Test peak radiation, Rad 1, top (kW/m^2)	Test peak radiation, Rad 2, bottom (kW/m^2)	Peak back face radiation (kW/m^2)	Peak front face temp. (°C)	Peak back face temp. (°C)	Time to flaming (s)	Failure mode	Glass failure 1st crack (s)
Film 1	Annealed	4	F	Rubber	F	4	5	4	2	110	105	No	Crack	230
Film 2	Annealed	4	G	Rubber	F	5	7	5	1	146	134	No	Crack	330
Film 3	Annealed	4	H	Rubber	F	6	8	6	2	154	138	No	Crack	355
Film 4	Annealed	4	F	Rubber	F	6	9	6	3	156	141	No	Crack	380
Film 10	Annealed	4	C	Rubber	F	6	8	6	3	145	141	No	Crack	370
Film 11	Annealed	4	C	Rubber	F	6	8	6	2	146	128	No	Crack	349
Film 12	Annealed	4	D	Rubber	F	15	23	15	3	217	164	No	Crack	510
Film 13	Annealed	4	D	Rubber	F	16	27	16	2	211	222	No	Crack	480
Film 5	Annealed	4	F	Rubber	F	6	7	6	3	149	135	No	Crack	350
Film 6	Annealed	4	F	Rubber	F	4	5	4	2	121	81	No	Crack	250
Film 7	Annealed	4	F	Rubber	F	3	5	3	2	112	104	No	Crack	210
Film 8	Annealed	4	G	Rubber	F	6	8	6	1	141	109	No	Crack	382
Film 9	Annealed	4	G	Rubber	F	7	9	7	1	146	116	No	Crack	398

Film 12 and 13 had external films, i.e. films were placed on the radiant panel side of the glass. All other tests were with internal film.

Correct application of these films to manufacturer's specifications is important, as is the recommended curing time. Specimens were allowed to cure for a minimum of three days, and the curing process was enhanced by placing the windows outside so that ultraviolet light would increase curing effectiveness, as was recommended by the manufacturer.

B3.2 Discussion of results

It can be seen from the front and back face temperatures for these two tests that the reflective qualities of these films, which have more of a metallic appearance than the other films, have a much reduced back face temperature – up to 100°C lower than other non-clear films. The same holds for front face temperatures. This is a plus in using films, as the reduction of radiation and heat to internal surfaces reduces the likelihood of components such as curtains igniting.

There was no flaming of any part of framing during these tests, however off-gasing of the film and frame componentry was present and, when not visible, could be smelt.

The failure mode of these films is such that they tend to shrink back from the edges on heating, exposing the glazing to which it was adhered. This also gives films the chance of peeling off from the glass. The shrink back then means the glass will act as if there is no film and glass cracking will propagate at the edges, which was a standard failure mode observed in this experimentation.

Figure B5 shows a standard failure mode for a film-coated aluminium window. The change in opaqueness of the films occurred in all tests as the plastics and other compounds that are incorporated in the film broke down on heating. In the figure, it can clearly seen where the film has peeled back from the edge at the bottom left corner of the window. This photo (from Film 11) also shows that the glass stayed intact in its frame even though the rubber beading melted.

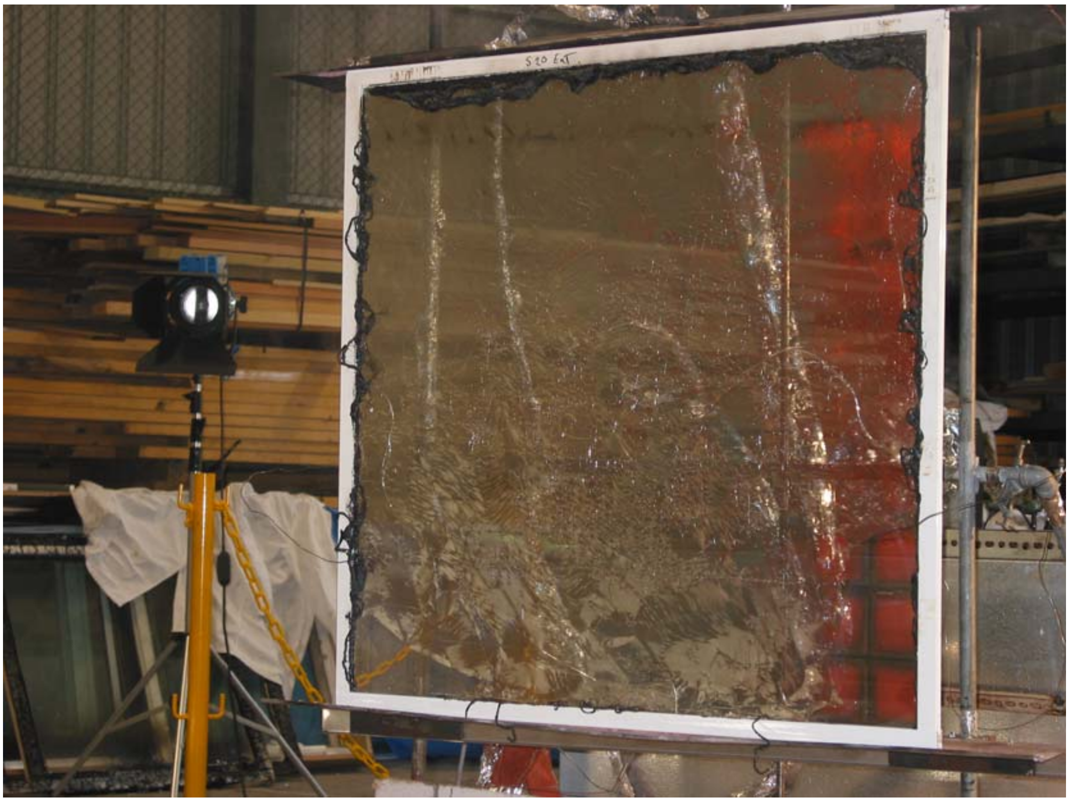

Figure B5. Film shrink back during radiation exposure.

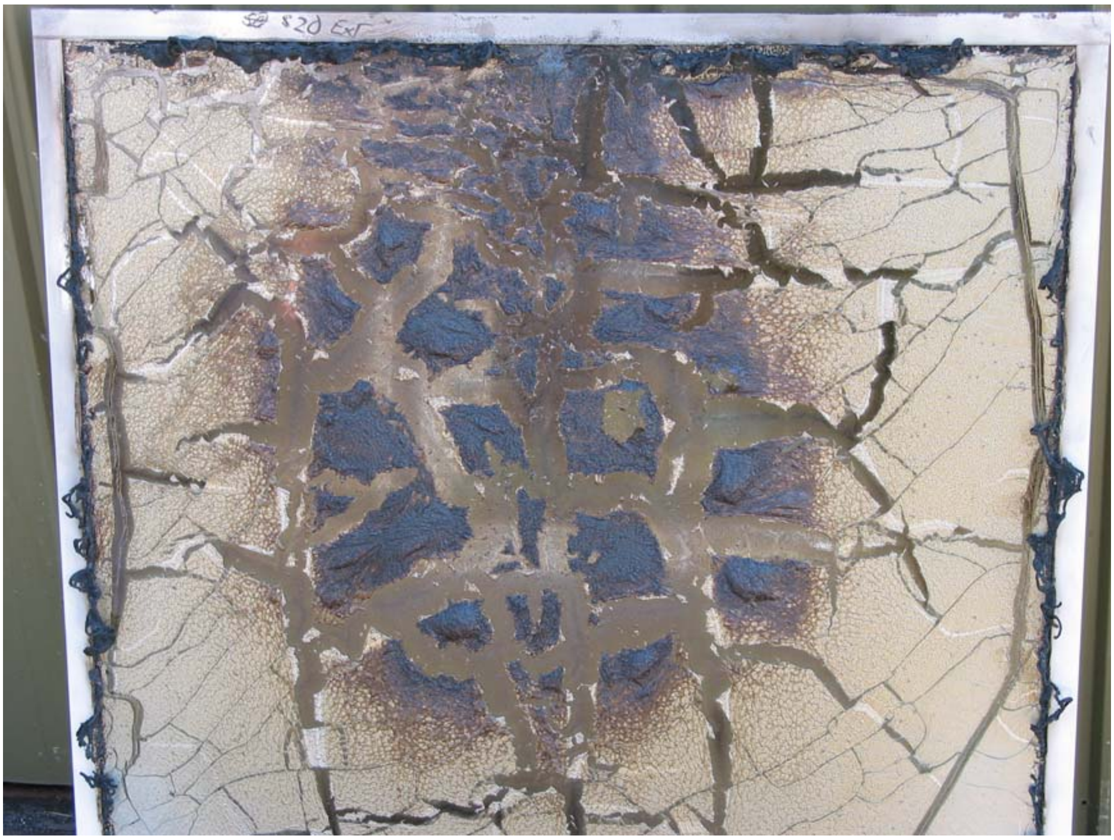

Figure B6. Crazing of metallic film after radiation exposure and cooling.

Appendix C – Suppliers Index

- All Weather Aluminium Windows and Doors, 237–239 Governor Road, Braeside, Victoria 3195, Australia (aluminium window frames and flyscreens).
- Bekaert Specialty Films Aust., PO Box 153, Chirnside Park, Victoria 3116, Australia (films).
- Canterbury Windows and Doors, 50 Osborne Avenue, Springvale, Victoria 3171, Australia (windows).
- Metal Mesh P/L, 14–16 Crawford Street, Braeside, Victoria 3195, Australia (stainless steel mesh).
- Moorabbin Glass P/L, 20 Station Road, Cheltenham, Victoria 3192, Australia (glass).
- Trend Windows and Doors P/L, 44–22 Mandoon Road, Girraween, NSW 2145, Australia (windows).
- Wacker Chemicals Aust. P/L, Unit 18/20 Duerdin Street, Clayton North, Victoria 3168, Australia (Elastosil M4470 high-temperature silicone).

Appendix D – Laboratory Condition Measurements

D1. Environmental Measurement

The environment in which testing was done was measured in various forms during the test methodology. The final method included two types of measurement.

In the first method, a relative humidity and temperature measurement meter was placed at the operator distance away from the radiant panel (approximately 6 m) at a height of 1.2 m. This device continuously logged data that was transmitted to each test data file through an RS232 communications port.

The second method employed was to measure the temperature around the front face and near the backface of the specimen.

In the second method, a K-type thermocouple was placed in a ceramic tube of 5 mm internal diameter. The thermocouple had wire tied around it leaving tags (spacers) so that, on insertion of the thermocouple in the tube, the thermocouple was spaced so it did not touch the sides of the tube and its tip was withdrawn into the tube 25 mm to minimise flame immersion. Air was drawn past the thermocouple at a very low flow rate using a vacuum pump.

The theory of using the second method was to draw air over the thermocouple to measure the convective temperature component. This is discussed further in Section 4.1.

Figure D1 shows typical measurements during a test. The data from these tests and its full analysis is yet to be done and the significance of any trends in the data is not fully understood at this stage. The measurement is, however, considered important and will be further scrutinised and reported as part of a research document at a later date.

As can be seen in Figure D1, the room temperature and back face aspirated thermocouple follow each other fairly closely until the point where the heat from the glass heating and obviously input from the radiant panel affected its measured temperature.

The difference between the front face top aspirated temperature and that of the front face top thermocouple gives an indication of the difference between the convective temperature measured by the aspirated thermocouple and that of the combined temperature effects measured by the top thermocouple.

Effectively the difference between these two measurements leaves only the conductive temperature component. The difficulty with this measure, however, is that thermocouples do heat along their length as well as their tip, so there is some measured component where the thermocouple is measuring its own heating. The degree of this is not discernable by measurement in this experimentation, but could be empirically categorised in future works.

The effect that ambient temperature has on the end result of glass breakage is unknown. The effect of temperature between back and front face glass and ambient temperatures is a complex issue.

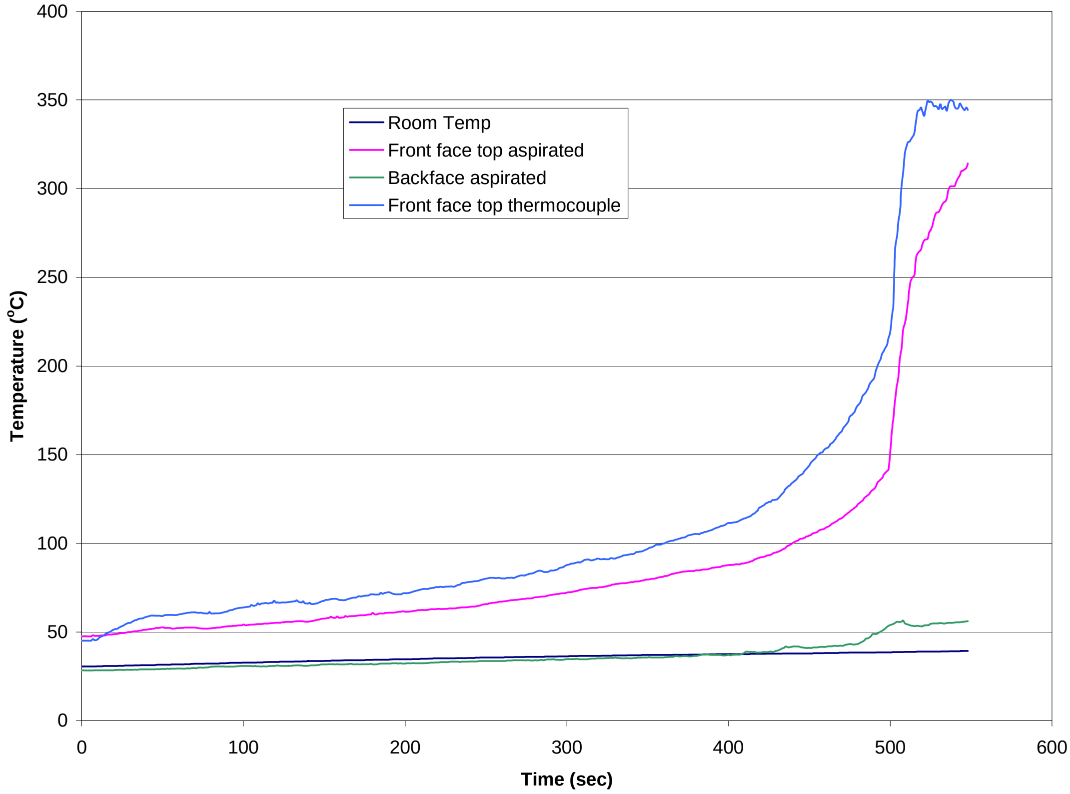

Figure D1. Laboratory temperatures versus test measured temperatures.